The Effect of Mechanical Deformations on the Radiation Patterns of Large Space-Based Arrays

G. M. SHAW
Electronics Research Laboratory
Laboratory Operations
The Aerospace Corporation
El Segundo, CA 90245

DTIC
ELECTE
MAR 2 0 1990
D

30 April 1988

Prepared for

AD-A219 288

This report was submitted by The Aerospace Corporation, El Segundo, CA 90245, under Contract No. F04701-85-C-0086-P00019 with the Space Division, P.O. Box 92960, Worldway Postal Center, Los Angeles, CA 90009-2960. It was reviewed and approved for The Aerospace Corporation by M. J. Daugherty, Director, Electronics Research Laboratory.

Lt Wesley R. Dotts/CWHB   was the project officer for the Mission-Oriented Investigation and Experimentation (MOIE) Program.

This report has been reviewed by the Public Affairs Office (PAS) and is releasable to the National Technical Information Service (NTIS). At NTIS, it will be available to the general public, including foreign nationals.

This technical report has been reviewed and is approved for publication. Publication of this report does not constitute Air Force approval of the report's findings or conclusions. It is published only for the exchange and stimulation of ideas.

WESLEY R. DOTTS, Lt, USAF
MOIE Project Officer
SD/CWHB

RAYMOND M. LEONG, Maj, USAF
Deputy Director, AFSTC West Coast Office
AFSTC/WCO OL-AB

REPORT DOCUMENTATION PAGE

1a. REPORT SECURITY CLASSIFICATION Unclassified	1b. RESTRICTIVE MARKINGS
2a. SECURITY CLASSIFICATION AUTHORITY	3. DISTRIBUTION/AVAILABILITY OF REPORT Approved for public release;
2b. DECLASSIFICATION/DOWNGRADING SCHEDULE	distribution unlimited.

4. PERFORMING ORGANIZATION REPORT NUMBER(S) TR-0086A(2925-05)-1	5. MONITORING ORGANIZATION REPORT NUMBER(S) SD-TR-88-49

6a. NAME OF PERFORMING ORGANIZATION The Aerospace Corporation Laboratory Operations	6b. OFFICE SYMBOL (If applicable)	7a. NAME OF MONITORING ORGANIZATION Space Division
6c. ADDRESS (City, State, and ZIP Code) El Segundo, CA 90245		7b. ADDRESS (City, State, and ZIP Code) Los Angeles Air Force Base Los Angeles, CA 90009-2960

8a. NAME OF FUNDING/SPONSORING ORGANIZATION	8b. OFFICE SYMBOL (If applicable)	9. PROCUREMENT INSTRUMENT IDENTIFICATION NUMBER F04701-85-C-0086-P00019

8c. ADDRESS (City, State, and ZIP Code)	10. SOURCE OF FUNDING NUMBERS			
	PROGRAM ELEMENT NO.	PROJECT NO.	TASK NO.	WORK UNIT ACCESSION NO.

11. TITLE (Include Security Classification)
The Effect of Mechanical Deformation on the Radiation
Patterns of Large Space-Based Arrays

12. PERSONAL AUTHOR(S)
Shaw, Gwendolyn M.

13a. TYPE OF REPORT	13b. TIME COVERED FROM _____ TO _____	14. DATE OF REPORT (Year, Month, Day) 1988 April 30	15. PAGE COUNT 61

16. SUPPLEMENTARY NOTATION

17	COSATI CODES		18. SUBJECT TERMS (Continue on reverse if necessary and identify by block number)
FIELD	GROUP	SUB-GROUP	Deployable antennas Phased array Random error
			Fourier series Probability theory Satellite antennas
			Integral equation Radiation pattern

19. ABSTRACT (Continue on reverse if necessary and identify by block number)

Large phased arrays for space applications require light-weight deployable structures. As these structures are not completely rigid, they undergo dynamic deformations in orbit that are typically expressed as mechanical modes of surface position. In contrast with conventional antenna tolerance theory, which is based on a random Gaussian representation of manufacturing tolerance, these deformations follow a deterministic function.

The effects of these mechanical deformations on the radiation performance of the phased array are analyzed. Closed-form solutions are presented for uniformly illuminated arrays, and results are shown for various mechanical modes. Tapered-amplitude array excitation is then treated numerically and contrasted with uniformly excited arrays. The array patterns resulting from modal errors and random errors are compared.

20. DISTRIBUTION/AVAILABILITY OF ABSTRACT [X] UNCLASSIFIED/UNLIMITED ☐ SAME AS RPT. ☐ DTIC USERS	21. ABSTRACT SECURITY CLASSIFICATION Unclassified	
22a. NAME OF RESPONSIBLE INDIVIDUAL	22b. TELEPHONE (Include Area Code)	22c. OFFICE SYMBOL

DD FORM 1473, 84 MAR   83 APR edition may be used until exhausted.
All other editions are obsolete.

CONTENTS

1

FIGURES

TABLES

I. INTRODUCTION

Previous analyses of antenna surface errors have assumed that errors are distributed randomly. Such random distribution is a reasonable model for manufacturing errors in a rigid structure such as an aluminum reflector antenna. However, as large space-based phased-array antennas must be both lightweight and deployable, they are consequently not rigid and thus undergo dynamic deformations in orbit. Because these deformations are typically expressed in terms of the mechanical modes of the structure, the errors in the array-element positions can be expressed discretely as mechanical modes of surface position. These mechanical deformations vary slowly with time, so that the radiation performance can be computed from a "frozen" mechanical deformation.

When the time-varying deformations are expressed as a sum of the mechanical modes weighted by their individual time-phased amplitudes, the radiation pattern of an array distorted by a single, "frozen" mechanical mode can be analyzed. In this way, the relationship between individual mechanical modes and the distorted radiation pattern can be observed. As the actual modal sum depends on the specific array design, single-mode analysis indicates those mechanical modes that should be optimized in the array design to minimize the pattern distortion.

Closed-form solutions for the radiation patterns of uniformly illuminated arrays having modal deformations are developed (1) for small-amplitude deformations, (2) in terms of Bessel functions at discrete angles, and (3) in terms of paired echoes of the undistorted array pattern; these solutions are compared with the antenna-tolerance theory developed by Ruze.[1] In addition, the pattern distortions for arrays having tapered illuminations are computed.

II. ANALYSIS OF MECHANICALLY DEFORMED ARRAYS

The array geometry illustrated in Fig. 1 is ideally planar in the x-y plane. Mechanical deformation results in element displacements in the plane and normal to the plane; however, the array pattern is decoupled from the in-plane displacements. Consequently, only the element displacements in the z-direction will be analyzed. At the far-field angle (θ,ϕ), the contribution of a single element, including its phase, is

$$V_i(\theta,\phi) = a_e(\theta,\phi)\exp\{jk[\sin\theta(x_i\cos\phi + y_i\sin\phi) + z(x_i,y_i)\cos\theta]\} \qquad (1)$$

where $a_e(\theta,\phi)$ is the pattern of a single element at the position $[x_i,y_i,z(x_iy_i)]$. The pattern of the array is the sum of the phase contributions of the individual elements:

$$V(\theta,\phi) = \sum_i A(x_i,y_i)\exp\{jk[\sin\theta(x_i\cos\phi + y_i\sin\phi) + z(x_iy_i)\cos\theta]\} \qquad (2)$$

where $A(x,y)$ is the illumination function. Generally, antenna patterns are computed for a particular plane of interest, and the geometry of the planar array is compressed into an equivalent linear array to compute that pattern conveniently. However, an additional assumption must be made to compress a planar array having element displacements that are normal to the array plane. For the pattern plane $\phi = (0^o,180^o)$, the normal displacements of the array elements are assumed to vary in the x direction only, and the illumination amplitudes are assumed to vary in the x direction, independently of y. The pattern of the equivalent linear array is

$$V(\theta) = \sum_i A(x_i)\exp\{jk[\pm x_i\sin\theta + z(x_i)\cos\theta]\} \qquad (3)$$

For a large array with close element spacing, the array pattern may be approximated by the integral

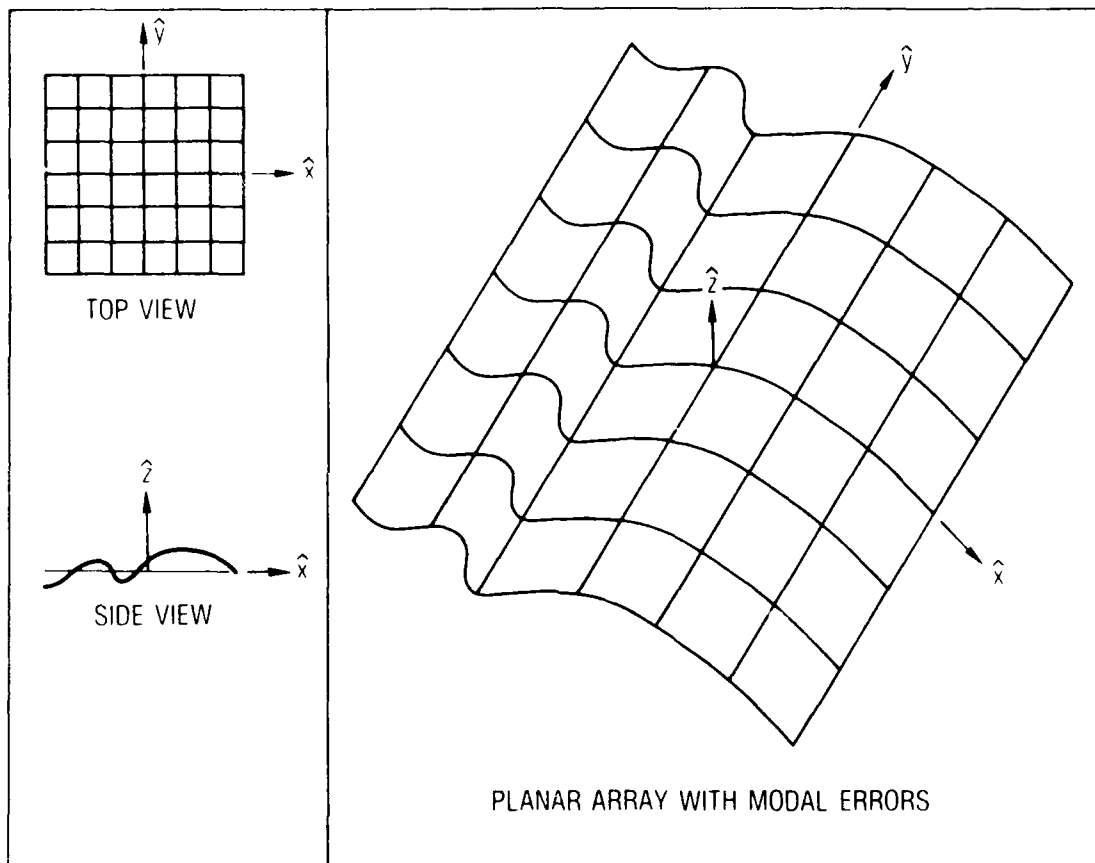$$V(\theta) = \int_{-L}^{L} A(x)\exp\{jk[\pm x\sin\theta + z(x)\cos\theta]\}dx \qquad (4)$$

Figure 1. Array Geometry with Oblique, Top, and Side Views
for a Deformed Rectangular, Planar Array

where 2L is the x dimension of the array. Sections II.A and B apply Eq. (4) to uniformly illuminated arrays having random and deterministic deformations.

A. RANDOM DEFORMATIONS

The standard antenna-tolerance theory developed by Ruze[1] models random surface errors as phase errors having a Gaussian density, then computes the radiation pattern and gain loss in a statistical sense. To compute the directivity in the more general case involving phase and amplitude errors, one must assume that the power density in a specific direction does not correlate with the total radiated power.[2] The random analysis is summarized for comparison with the deterministic-error model.

Ruze defines the amplitudes of the surface errors by two functions: (1) the Gaussian probability-density function, and (2) a correlation function. The Gaussian function specifies the density of phase-error values, and the correlation function specifies the likelihood that two phase errors on different sections of the surface will have equal values. Ruze suggests several forms of correlation functions, the simplest being the "hat box." The hat-box correlation function, illustrated in Fig. 2, is a pulse function that has the value 1 in a correlation region and the value 0 outside that region; within the correlation region the values are equal, and outside the region they are uncorrelated.

As the phase-error values are proportional to the deformation amplitudes of the array, one can extend this tolerance theory to the phase-error values generated by the mechanical deformations of large arrays; this can be achieved by assigning a representative Gaussian probability-density function and an appropriate correlation function to the deformation amplitudes. The probabilistic expectation of the far-field radiated power may be obtained by multiplying the radiated power, which is a function of the array element positions, by the probability density of the deformation amplitudes and integrating over the possible amplitudes. The expression for the expectation is

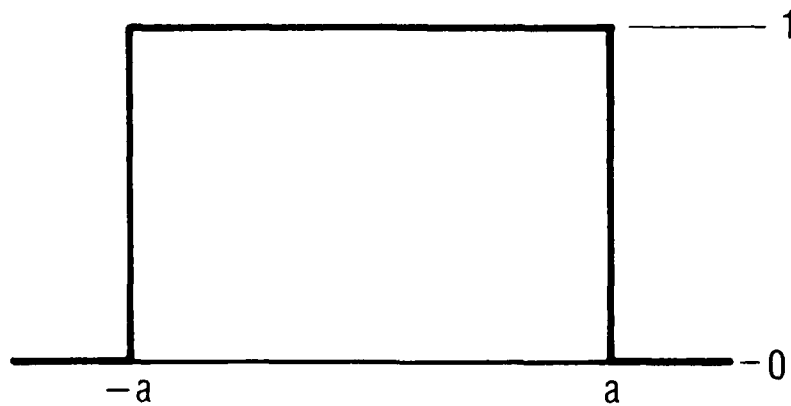$$E\{P(\theta)\} = \int_{-\infty}^{\infty} P(\theta, z-z')f(z-z')d(z-z') \tag{5}$$

9

Figure 2.   "Hat Box" Function for the Correlation of Surface-Error
Amplitudes Having a Correlation Region of Dimension 2a

where z and z' are the deformation amplitudes at positions x and x', $P(\theta, z-z')$ is the product of the voltage and its complex conjugate, and $f(z-z')$ is the Gaussian probability-density function, with zero mean and σ^2 variance. For a hat-box correlation function whose correlation-region dimension of 2a is much smaller than the array dimension 2L, the expression for the expected power of a uniformly illuminated array is

$$E\{P(\theta)\} = (2L)^2 \ \{[\frac{\sin(kL\sin\theta)}{kL\sin\theta}]^2 \ e^{-k^2\sigma^2\cos^2\theta}$$

$$+ \ \frac{a}{L} \ \frac{\sin(ka\sin\theta)}{ka\sin\theta} \ [1- \ e^{-k^2\sigma^2\cos^2\theta}]\} \qquad (6)$$

The above expression has two terms. One term is the undistorted radiation pattern reduced by an exponential function, and the other term is directly related to the ratio of the size of the correlation region to the length of the array. If the correlation region, 2a, is much smaller than the length of the array, only the first term of the expected power is significant. In this case, the radiated power decreases exponentially with an increase in the variance of z.

An array having Gaussian random deformations and a small correlation interval has a radiation pattern whose gain decreases uniformly, as shown in Fig. 3. The radiation patterns of arrays having modal deformations have nonuniform changes in gain.

B. DETERMINISTIC DEFORMATIONS

A large space-based array will have slow mechanical oscillations. At any instant in time, the continuous surface that spans the element positions can be expressed as a deterministic function. The instantaneous element displacements from the plane can be expressed as a sum of fundamental modes. The fundamental modes satisfying the Dirichlet boundary conditions are odd-order cosine and even-order sine modes:
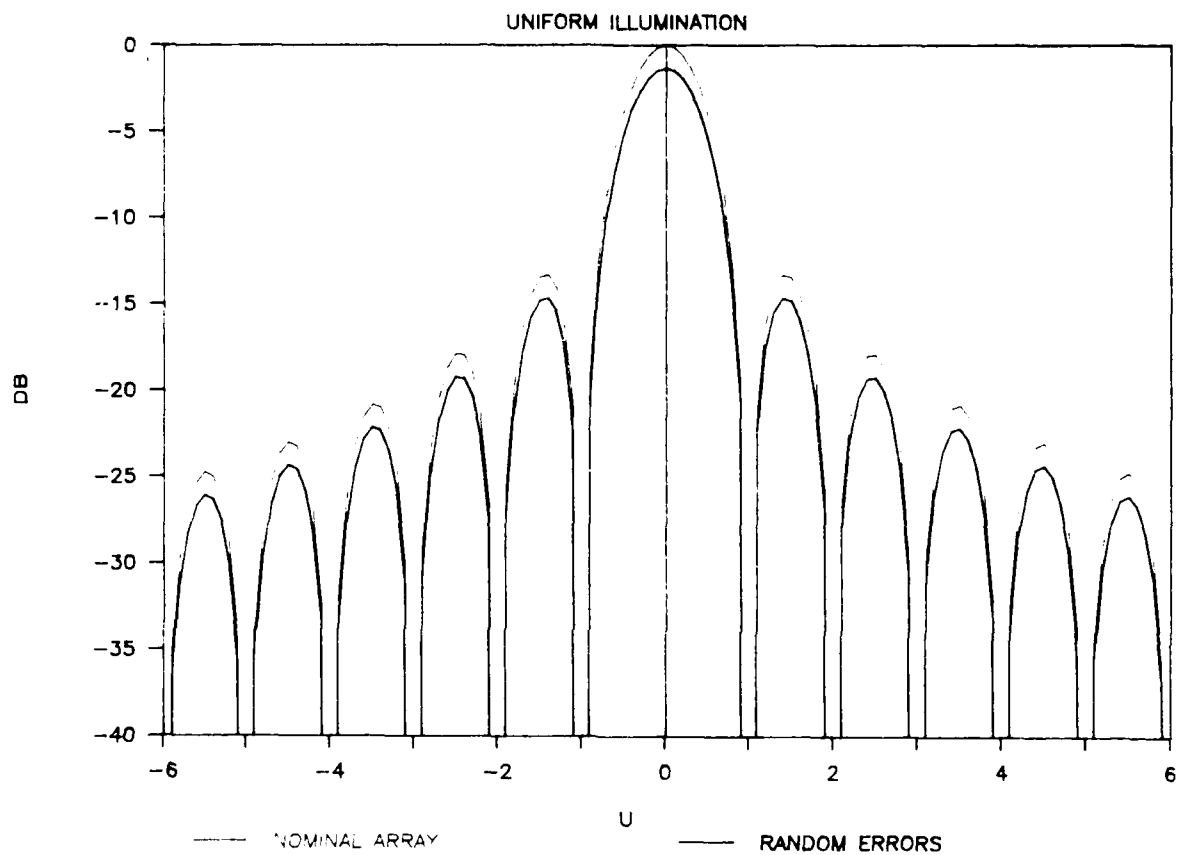
Figure 3. Radiation Pattern of a Large Array Having Random Gaussian Element-Position Errors ($\sigma^2 = 0.03\lambda^2$, $2L = 100\lambda$)

$$z(x) = \sum_{m=1}^{\infty} \left(a_{2m-1} \cos\frac{(2m-1)\pi x}{2L} + b_{2m} \sin\frac{2m\pi x}{2L} \right) \qquad (7)$$

The fundamental modes satisfying Neumann boundary conditions are even-order cosine and odd-order sine modes:

$$z(x) = a_0 + \sum_{m=1}^{\infty} \left(a_{2m} \cos\frac{2m\pi x}{2L} + b_{2m-1} \sin\frac{(2m-1)\pi x}{2L} \right) \qquad (8)$$

This section reviews three solutions to the radiation-pattern integral for a uniformly illuminated, linear array having single-mode errors. One solution is approximate for small-amplitude errors, the second is exact for discrete angles, and the third is exact in terms of an infinite summation of paired echoes. Numerical solutions computed by means of Simpson's rule are shown in Appendix B.

1. SMALL-AMPLITUDE APPROXIMATION

The small-amplitude solution uses the truncated-series approximation for the exponential function $e^x \approx 1 + x$. The new integral is integrable to the sum of the ideal pattern, $\sin\pi u/\pi u$, and a small error pattern,

$$V(u) \quad 2L\,\frac{\sin\pi u}{\pi u} + j\pi u'\,\frac{1}{L} \int_{-L}^{L} z(x)\,\exp\left(\pm\, j\pi u\,\frac{x}{L}\right)\,dx \qquad (9)$$

where $z(x)$ is either a sine or a cosine mode of any order and u is defined as follows:

$$\pi u = kL\sin\theta \qquad (10)$$

The pattern for an array having small-amplitude cosine errors is

$$V(u) \approx 2L\,\frac{\sin\pi u}{\pi u} + j\pi u'2a_n\left\{ \frac{\pi u\,\cos\frac{n\pi}{2}\,\sin\pi u}{\left(\frac{n\pi}{2}\right)^2 - (\pi u)^2} + \frac{\frac{n\pi}{2}\,\sin\frac{n\pi}{2}\,\cos\pi u}{\left(\frac{n\pi}{2}\right)^2 - (\pi u)^2} \right\} \qquad (11)$$

13

The pattern for an array having small-amplitude sine errors is

$$V(u) \simeq 2L \frac{\sin \pi u}{\pi u} \pm \pi u' 2b_n \left\{ \frac{\frac{n\pi}{2} \cos\frac{n\pi}{2} \sin \pi u}{\left(\frac{n\pi}{2}\right)^2 - (\pi u)^2} - \frac{\pi u \sin\frac{n\pi}{2} \cos \pi u}{\left(\frac{n\pi}{2}\right)^2 - (\pi u)^2} \right\} \qquad (12)$$

The denominator of the error terms, $\left(\frac{n\pi}{2}\right)^2 - (\pi u)^2$, yields removable singularities at $u_s = \pm \frac{n}{2}$, and a $1/u$ or $1/u^2$ taper for $u < -|u_s|$ and $u > |u_s|$. Therefore, the error terms (see Figs. 4-7) have maxima for values of u in the vicinities of $+\frac{n}{2}$ and $-\frac{n}{2}$. For sine errors the error term is odd (i.e., asymmetric) about $u = 0$; thus the error pattern adds to the ideal pattern around $u = +\frac{n}{2}$, and subtracts from the ideal pattern around $u = -\frac{n}{2}$, producing an asymmetric pattern. For cosine errors the error terms are even (i.e., symmetric) about $u = 0$, so the total pattern is symmetric; however, the error term has nonzero values at the nulls of the ideal pattern, so the total pattern has filled-in nulls.

2. DISCRETE-ANGLE SOLUTION

The integral for the radiation pattern of a uniformly illuminated line source having single, even-mode deformations has a form similar to the integral representation of the Bessel function of the first kind (integer order):

$$J_m(z) = \frac{1}{\pi} \int_0^\pi \cos(z \sin \gamma - m\gamma) \, d\gamma \qquad (13)$$

The transformation of Eq. (4) for an even-sine mode into the form of Eq. (12) yields

$$V(u) = \frac{2L}{n\pi} \int_{-\frac{n\pi}{2}}^{\frac{n\pi}{2}} \exp\left[j\left(\pm \frac{2u}{n}\eta + \pi u' \frac{b_n}{L} \sin \eta\right) \right] d\eta \qquad (14)$$

The variable transformation for the order of the Bessel function is a function of the far-field angle. Therefore, the solution for the radiation pattern in terms of Bessel functions of integer order is valid only at the angles for
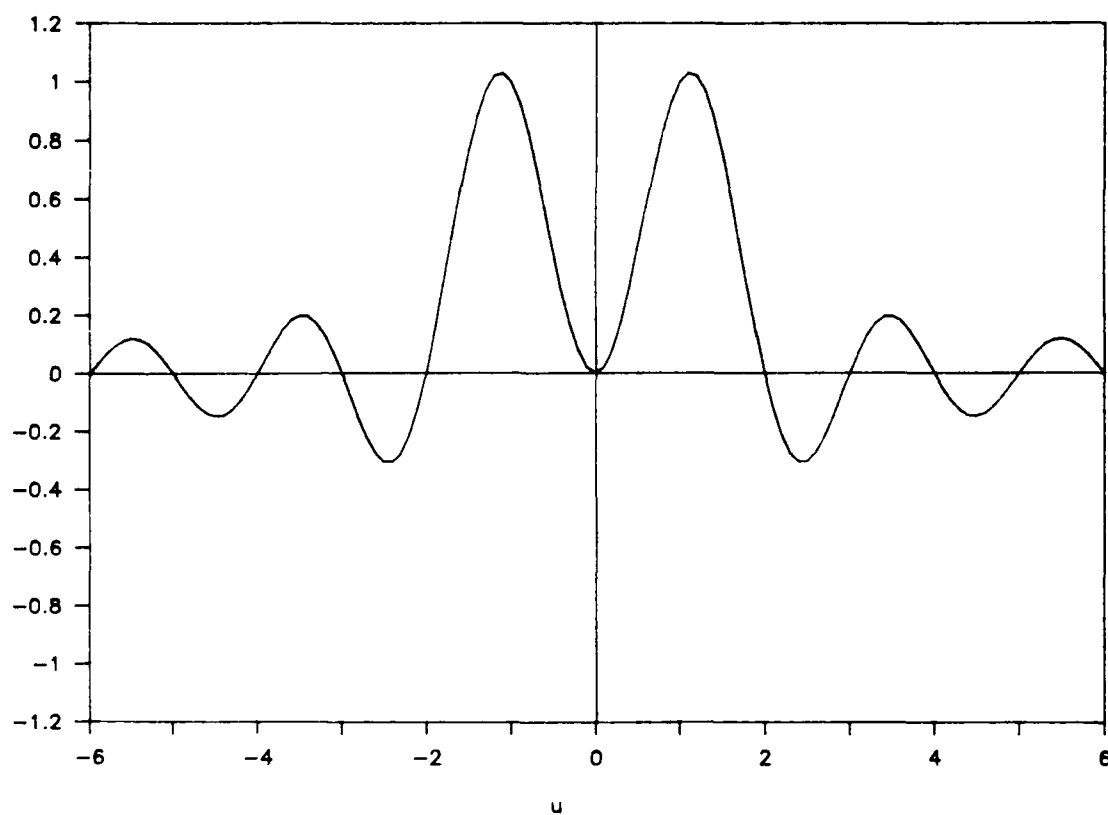
14

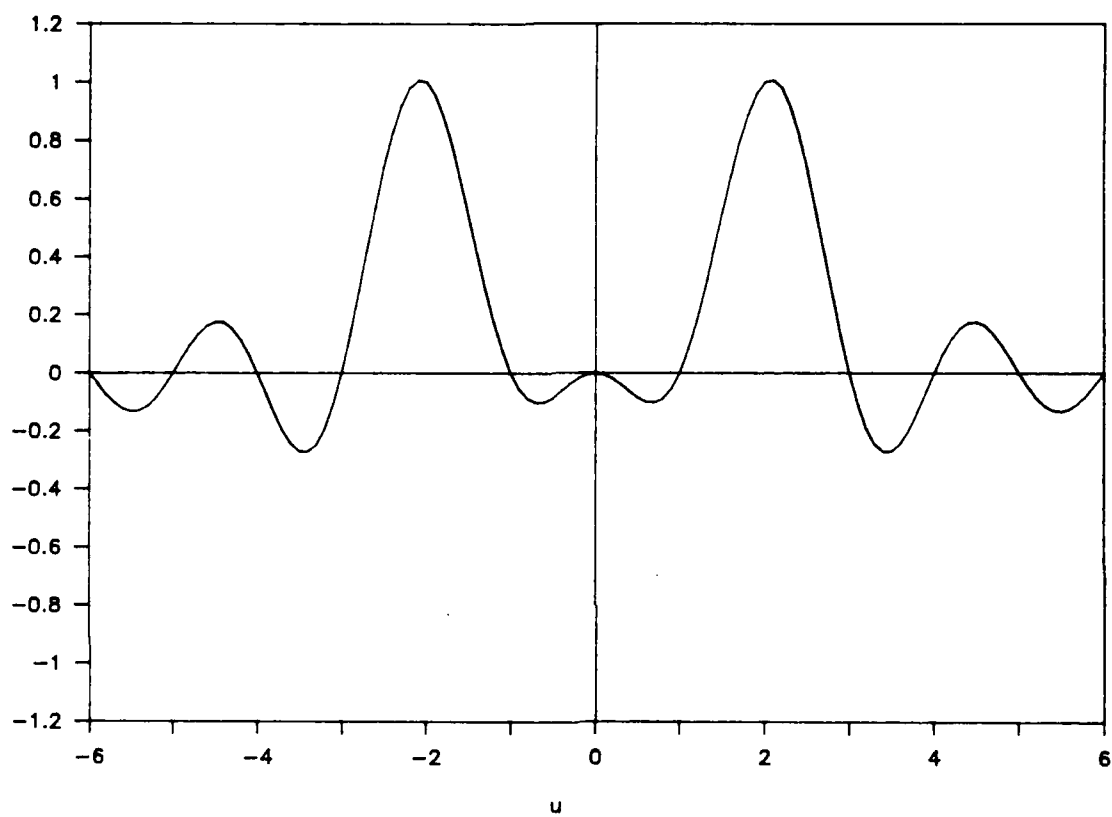Figure 4. Error Term for the Small-Amplitude Approximation of the $n = 1$ Cosine Mode Normalized to $ka_1\cos\theta$

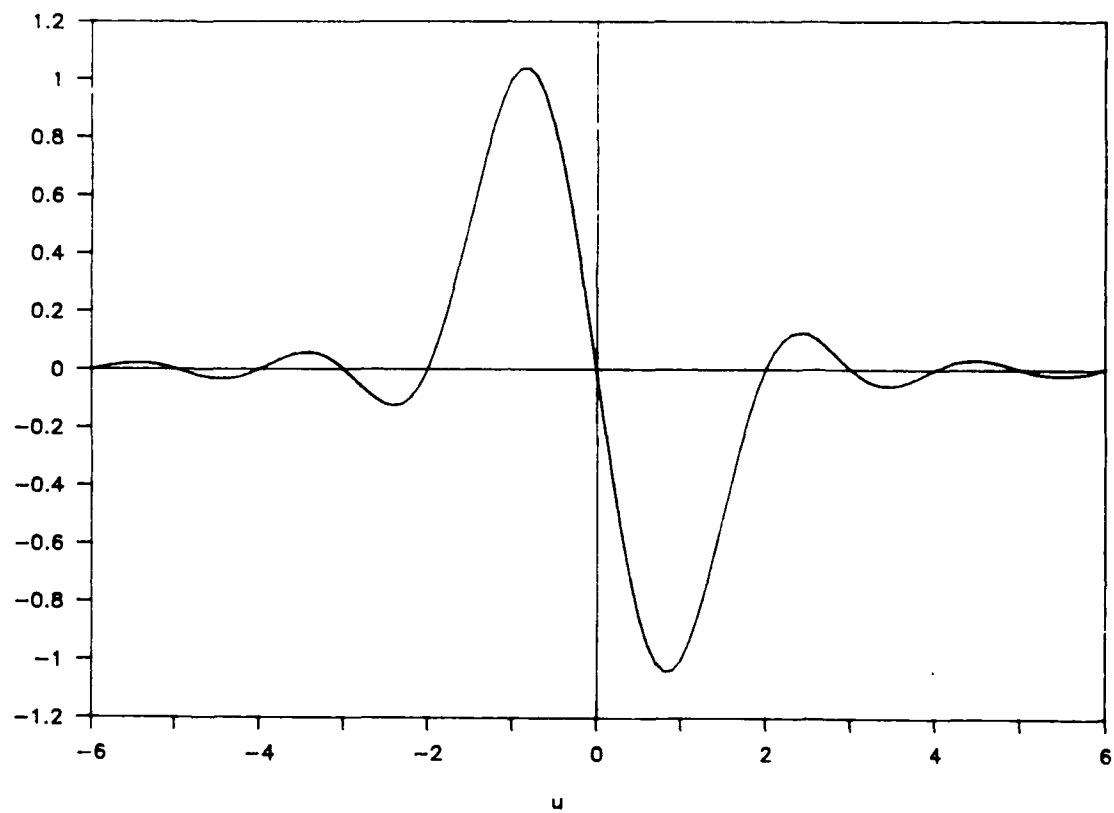Figure 5. Error Term for the Small-Amplitude Approximation of the $n = 2$ Cosine Mode Normalized to $ka_2\cos\theta$

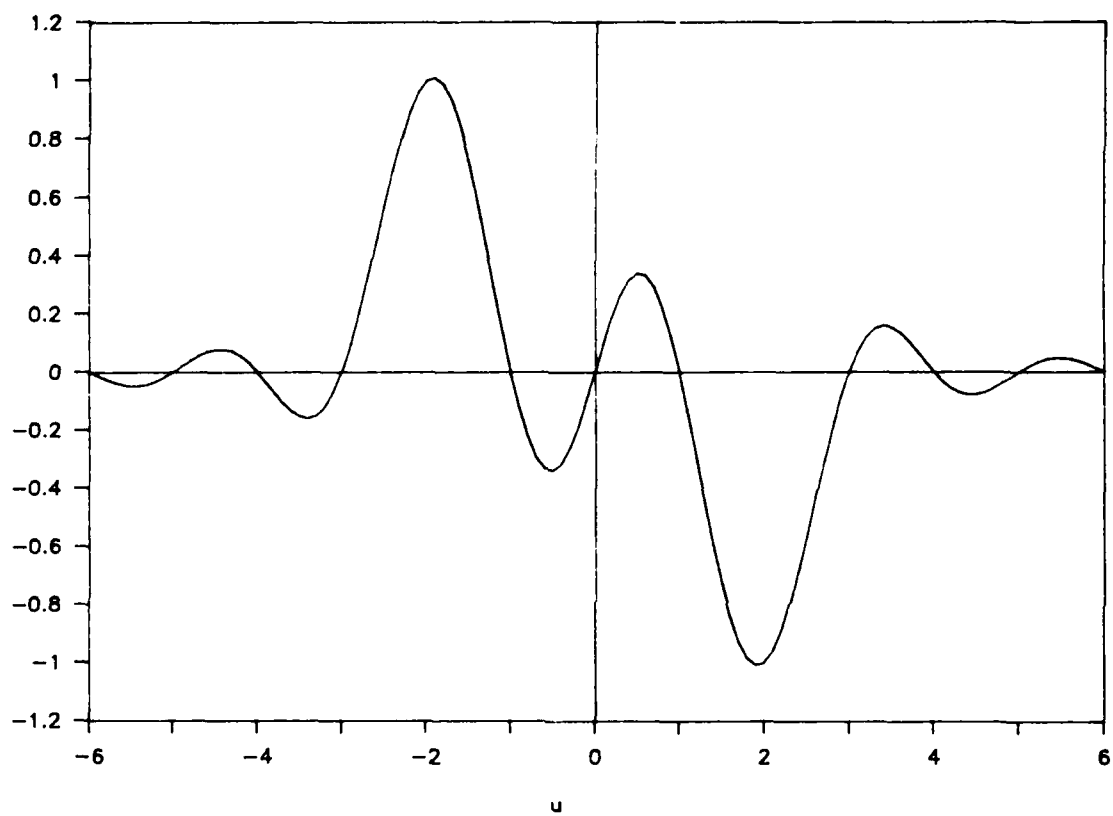Figure 6. Error Term for the Small-Amplitude Approximation of the n = 1 Sine Mode Normalized to $kb_1\cos\theta$

17

Figure 7.   Error Term for the Small-Amplitude Approximation of
the n = 2 Sine Mode Normalized to $kb_2 \cosh$

which 2u/n takes on integer values. The details for the development of this discrete-angle solution are presented in Appendix A.

3. PAIRED-ECHO ANALYSIS

The paired echo is an intuitive method of understanding the distortion of a Fourier transform process such as might serve as a model for a filter or, in this case, a far-field pattern. Wheeler[6] uses a filter to describe the interpretation of amplitude and phase errors. In this example, the process is a Fourier transformation from the frequency domain of the signal, where the filter works, to the time domain of the signal. Amplitude and phase errors in the frequency domain translate to paired echoes of the signal in the time domain. The echoes from amplitude errors are equal in absolute value and sign, and are symmetrically placed about the signal (a positive pair); the echoes from phase errors are equal in absolute value, are opposite in sign, and are symmetrically placed about the signal (a negative pair). Positive and negative pairs are illustrated in Figs. 8 and 9.

The far-field pattern of an antenna is a Fourier transform of the aperture fields. Modal deformations of the aperture surface produce paired echoes in the far-field pattern. For an array having an illumination function that is even about the center of the array, the sine errors produce positive and negative pairs in the far field and the cosine errors produce only posi-tive pairs. Negative pairs contribute to an asymmetric pattern because they subtract from the ideal pattern on one side and add to it on the other.

For a uniformly illuminated array having single-mode errors, the paired echoes are expressed as follows.

For cosine errors the far-field pattern expressed in terms of its paired echoes is

$$V(u) = J_0\left(\pi u' \frac{a_n}{L}\right)\left[V_0(u) + \sum_{k=1}^{\infty} (-1)^k \frac{J_{2k}\left(\pi u' \frac{a_n}{L}\right)}{J_0\left(\pi u' \frac{a_n}{L}\right)} [V_0(u+kn) + V_0(u-kn)]\right.$$

$$\left. + j \sum_{k=0}^{\infty} (-1)^k \frac{J_{2k+1}\left(\pi u' \frac{a_n}{L}\right)}{J_0\left(\pi u' \frac{a_n}{L}\right)} \left\{V_0\left[u+\left(k+\frac{1}{2}\right)n\right] + V_0\left[u-\left(k+\frac{1}{2}\right)n\right]\right\}\right] \quad (15)$$
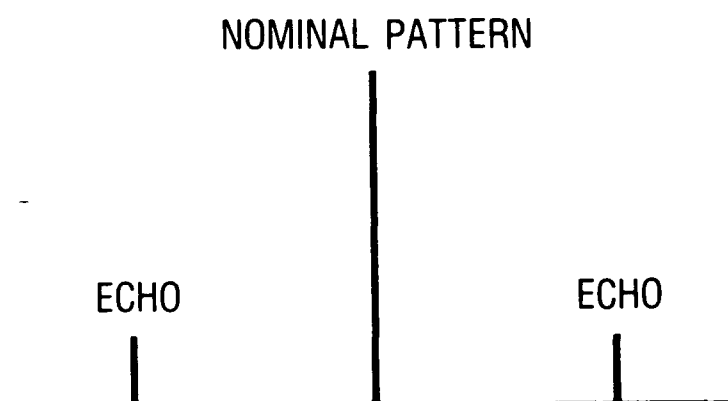
19

NOMINAL PATTERN

ECHO

ECHO

Figure 8.   Positive Pair

NOMINAL PATTERN

ECHO

ECHO
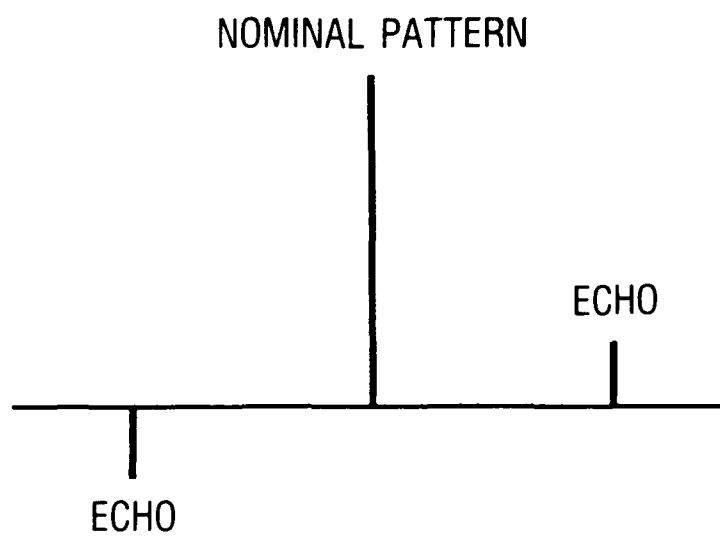
Figure 9. Negative Pair

For sine errors the far-field pattern expressed in terms of its paired echoes is

$$V(u) = J_0\left(\pi u' \frac{a_n}{L}\right)\left[V_0(u) + \sum_{k=1}^{\infty} \frac{J_{2k}\left(\pi u' \frac{a_n}{L}\right)}{J_0\left(\pi u' \frac{a_n}{L}\right)} \left[V_0(u+kn) + V_0(u-kn)\right]\right.$$

$$\left. + \sum_{k=0}^{\infty} \frac{J_{2k+1}\left(\pi u' \frac{b_n}{L}\right)}{J_0\left(\pi u' \frac{b_n}{L}\right)} \left\{V_0\left[u+\left(k+\frac{1}{2}\right)n\right] - V_0\left[u-\left(k+\frac{1}{2}\right)n\right]\right\}\right] \tag{16}$$

where $V_0(u)$ is the ideal array pattern. $V_0(u+u_e) + V_0(u-u_e)$ is a positive pair and $V_0(u+u_e) - V_0(u-u_e)$ is a negative pair. The radiation pattern for an array having an illumination function that is expressed as a Fourier series of position on the array may be similarly expressed in terms of paired echoes. The first two echoes for the $n = 1$ cosine and sine modes are illustrated in Figs. 10 and 11.
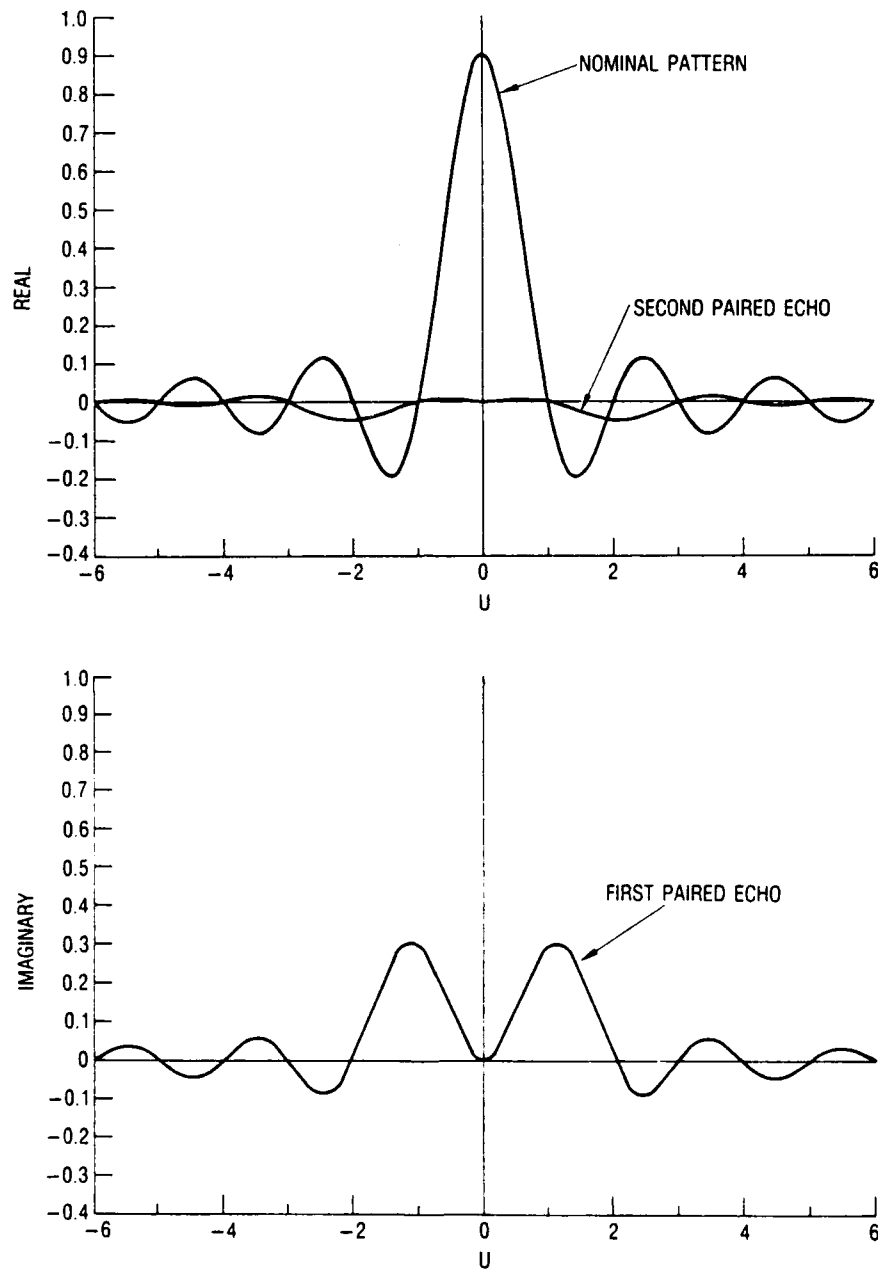
22

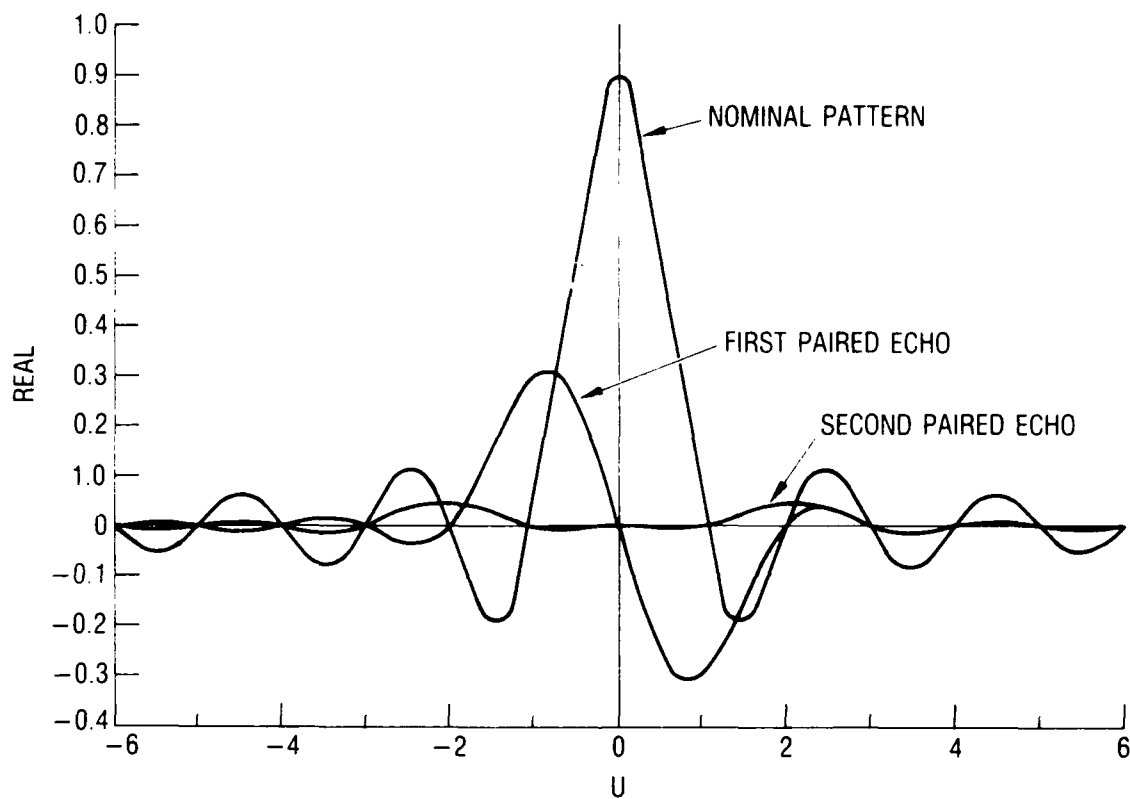Figure 10. The First Two Paired Echoes of the n = 1 Cosine Mode

Figure 11.   The First Two Paired Echoes of the n = 1 Sine Mode

III. PATTERN DISTORTION

The quality of the radiation pattern of an array depends upon the coherent interference of the contributions of the individual array elements. The phase errors due to the displacement of elements from the plane degrade the pattern quality, which is measured by (1) the gain, shape, beamwidth, and pointing accuracy of the main beam; (2) the sharpness of the nulls; and (3) the height of the innermost sidelobes. As was shown in Section II.A, random errors on a large array will effectively reduce the amplitude of the radiated power at all the far-field angles, thereby affecting the gain but not other qualities of the pattern. Single-mode errors have distinctive effects on the radiation pattern, as is suggested by the form of the small-amplitude approximation and as illustrated in Appendix B.

The effect of sine errors on the radiation pattern is a shifted boresight and an asymmetric pattern having higher sidelobes on one side of the main beam than on the other. The shifted boresight is explained by the linearity of the sine function at the origin, or the center of the array, which translates to linear phase errors; linear phase errors, in turn, steer the main beam to an angle that depends upon the peak amplitude of the errors. The asymmetry is due to the odd (i.e., asymmetrical) nature of the sine function. For the mode order $n = 1$, the main beam retains its gain, shape, and beamwidth, and the nulls retain their sharpness; however, the higher-order modes lose gain in the main beam and the nulls begin to fill in.

The effect of cosine errors on the radiation pattern is filled-in nulls and raised sidelobes. The filled-in nulls cause the first sidelobes to become part of the main beam. For large-amplitude errors, the main beam bifurcates when the edges of the array become out of phase with respect to the central portion of the array.

IV. ILLUMINATION TAPERS

Some applications requiring low sidelobes use arrays having tapered illumination functions. Single-mode errors, cosine modes in particular, raise the sidelobes of arrays having tapered illuminations, much as they raise the sidelobes of uniformly illuminated arrays. In order to meet the low-sidelobe requirement while compensating for expected modal errors, deformable arrays should be designed to have even lower sidelobes than would be the case for an ideal array in which deformation does not occur. One can prevent some effects of modal deformations of small order and amplitude by illuminating the array nonuniformly. In particular, the broadening of the main beam may be minimized by means of a cosine illumination function. A beamwidth factor can be used to evaluate illumination functions according to the degree to which they minimize beam broadening. Data for the ideal pattern are listed in Table 1. The beamwidth factor, which is defined as

$$BWF = 100 \left(\frac{BEAMWIDTH \ OF \ DISTORTED \ PATTERN}{BEAMWIDTH \ OF \ NOMINAL \ PATTERN} - 1 \right) \tag{17}$$

is used in Tables 2 through 4 to compare the success of several illumination functions for errors of equal amplitude and mode.

The uniform, triangular, and cosine illumination functions illustrated in Figs. 12 through 14 were evaluated. Using the beam-broadening factor of the uniform illumination function as a benchmark, the triangular illumination function and the first- and second-power cosine illumination functions have poor beam-broadening factors, and the higher-power cosine illumination functions have good ones. However, the ideal beamwidths of the higher-power cosine functions are large. In general, the beam broadening that results from single-mode errors is less for illumination functions that produce patterns having very low sidelobes than it is for illumination functions that produce patterns having moderately low sidelobes. The numerical solutions to the radiation patterns of arrays having tapered illuminations and single-mode errors are shown in Appendix B.

Table 1. Pattern Data for Arrays Having Uniform, Triangular, and Cosinusoidal Illumination Tapers and No Errors

	Uniform	Triangular	Cosine^1	Cosine^2	Cosine^3	Cosine^4	Cosine^5	Cosine^6	Cosine^7	Cosine^8
GAIN (dB)										
Main Beam	0.0	-6.0	-3.9	-6.0	-7.4	-8.5	-9.4	-10.1	-10.7	-11.3
First Sidelobe	-13.3	-32.6	-26.9	-37.5	-46.7	-55.3	-63.4	-70.9	-78.3	-86.2
PATTERN										
Half-power Beamwidth (degrees) Normalized to 2L/λ	50.6	73.0	68.0	82.4	94.9	106	116	125	134	142
Sidelobe Gain (dB) Referenced to the main beam	13.3	26.6	23.0	31.5	39.3	46.8	54.0	60.8	67.6	74.9

Table 2. Pattern Data for Arrays Having Uniform, Triangular, and Cosinusoidal Illumination Tapers and 0.25λ Sine Errors

	Uniform	Triangular	Cosine^1	Cosine^2	Cosine^3	Cosine^4	Cosine^5	Cosine^6	Cosine^7	Cosine^8
GAIN (dB)										
Main Beam	-0.1	-6.0	-4.0	-6.0	-7.5	-8.5	-9.4	-10.1	-10.7	-11.3
First Sidelobe, φ = 180° cut	-17.8	-32.4	-37.6	-58.5	-62.9	-73.0	-94.7	-92	-98	
First Sidelobe, φ = 0° cut	-10.4	-32.6	-22.1	-30.9	-38.6	-45.6	-52.2	-58.6	-64.7	-70.8
PATTERN										
Boresight Shift (degrees) Normalized to 2L/λ	34	39	38	40	41	41	42	42	42	43
Half-power Beamwidth (degrees) Normalized to 2L/λ	50.8	73.2	68.3	82.6	95.0	106	116	126	134	142
Sidelobe Gain (dB) Referenced to the main beam	10.3	26.4	18.1	24.9	31.1	37.1	42.8	48.5	54.0	59.5
Beamwidth Factor	0.32	0.41	0.38	0.29	0.17	0.11	0.09	0.06	0.04	0.02

Table 3.   Pattern Data for Arrays Having Uniform, Triangular, and Cosinusoidal Illumination Tapers and 0.50λ Sine Errors

	Uniform	Triangular	Cosine^1	Cosine^2	Cosine^3	Cosine^4	Cosine^5	Cosine^6	Cosine^7	Cosine^8
GAIN (dB)										
Main Beam	-0.3	-6.2	-4.1	-6.1	-7.5	-8.6	-9.4	-10.1	-10.7	-11.3
First Sidelobe, φ = 180° cut	-28.7	-34.7	-37.0	-49	-48					
First Sidelobe, φ = 0° cut	-8.5	-26.4	-19.0	-26.9	-33.7	-40.0	-45.9	-51.6	-57.0	-62.4
PATTERN										
Boresight Shift (degrees) Normalized to 2L/λ	70	76	76	79	81	82	84	84	85	85
Half-power Beamwidth (degrees) Normalized to 2L/λ	51.3	74.2	69.0	83.3	95.5	106	116	126	134	142
Sidelobe Gain (dB) Referenced to the main beam	8.2	20.2	14.9	20.8	26.2	31.4	36.5	41.5	46.3	51.1
Beamwidth Factor	1.20	1.67	1.50	1.09	0.70	0.46	0.32	0.22	0.15	0.11

Table 4. Pattern Data for Arrays Having Uniform, Triangular, and Cosinusoidal Illumination Tapers and 0.25λ Cosine Errors

	Uniform	Triangular	Cosine^1	Cosine^2	Cosine^3	Cosine^4	Cosine^5	Cosine^6	Cosine^7	Cosine^8
GAIN (dB)										
Main Beam	-1.0	-6.5	-4.4	-6.3	-7.6	-8.7	-9.5	-10.2	-10.8	-11.3
First Sidelobe	-9.6	-35.1	-22.3	-31.2	-32	-46	-54	-60	-67	
PATTERN										
Half-power Beamwidth (degrees) Normalized to 2L/λ	53.7	78.1	72.2	86.2	98.0	109	118	127	136	144
Sidelobe Gain (dB) Referenced to the main beam	8.6	28.6	17.9	24.9						
Beamwidth Factor	6.02	7.00	6.22	4.58	3.33	2.51	1.95	1.54	1.26	1.04
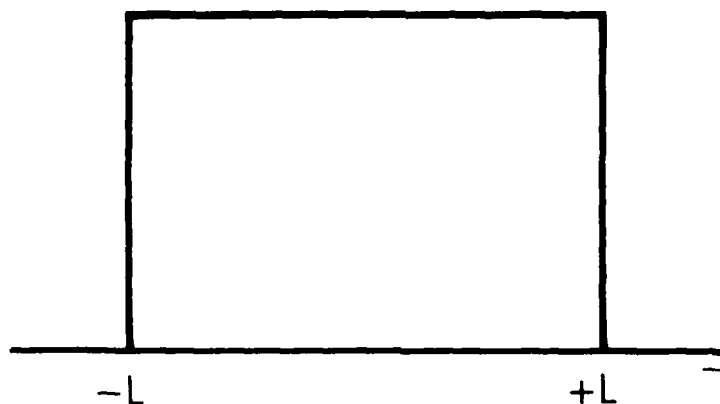
Figure 12. Uniform Illumination Function
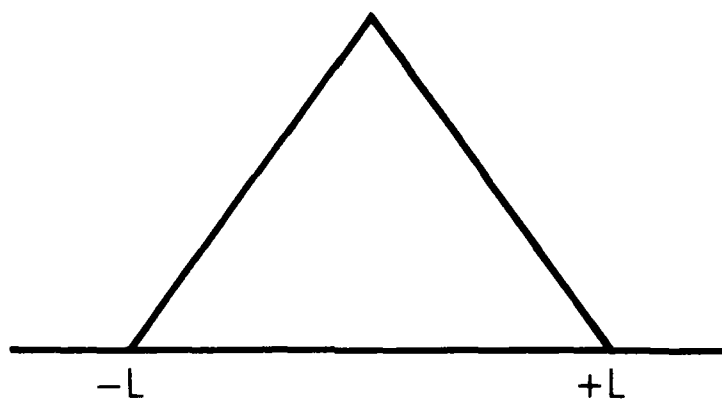
Figure 13.   Triangular Illumination Function
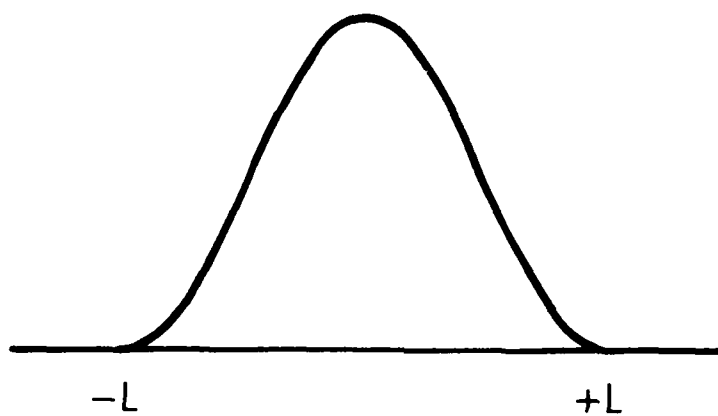
Figure 14. Cosinusoidal Illumination Function

V. SUMMARY

Instantaneous mechanical deformations of a large, oscillating planar array may be expressed by mechanical modes. The pattern distortion corresponding to single-mode deformations has distinct characteristics that differentiate it from random deformations that yield a uniform decrease in gain. This report offers several interpretations of this pattern distortion.

The small-amplitude approximation expresses the total pattern as a sum of the ideal pattern and an error pattern. One can determine the regions of the pattern for which the error term is significant by inspecting the error term. In these regions, the characteristics of the pattern distortion are dictated by whether the error pattern subtracts from or adds to the ideal pattern. When the small-amplitude approximation is used to find a numerical representation of the total pattern, the discrete-angle solution may be used to measure the accuracy of the results.

The paired-echo interpretation offers a perspective of the pattern distortion as pairs of echoes of the ideal pattern. The paired-echo analysis offers an intuitive interpretation of the pattern distortion by directly indicating the regions in which the echoes either add to or subtract from the ideal pattern.

Aperture-illumination functions that lower the sidelobes are typically used for applications requiring selective coverage. Modal deformations will cause pattern distortion that raises the sidelobes, broadens the main beam, and shifts the boresight by predictable amounts. The technique reported here, which uses the beamwidth factor to compare the robustness of several illumination functions, may be used to select an illumination function that compensates for the raised sidelobes caused by the predicted modal deformations of the array.

35/36

REFERENCES

1. J. Ruze, "Antenna Tolerance Theory -- A Review," Proc. IEEE 54, 633-640 (April 1966).

2. R. H. Ott and R. B. Dybdal, Statistics for the Directivity of an Antenna Array, Aerospace Technical Report No. ATR-84(8502)-1 (1984).

3. R. S. Elliott, Antenna Theory and Design (Englewood Cliffs, N.J.: Prentice Hall, Inc., 1981), Chap. 4.

4. S. Silver, "Aperture Illumination and Antenna Patterns," in Microwave Antenna Theory and Design (New York, N.Y.: McGraw-Hill Book Co., Inc., 1949), Chap. 6.

5. D. Barton and H. Ward, "Antenna Patterns and Illumination Functions," in Handbook of Radar Measurement, (Englewood Cliffs, N.J.: Prentice Hall, Inc., 1969), Appendix A.

6. H. A. Wheeler, "The Interpretation of Amplitude and Phase Distortion in Terms of Paired Echoes," Proc. IRE 27, 359-385 (June 1939).

7. A. Papoulis, The Fourier Integral and its Applications (New York, N.Y.: McGraw-Hill Book Co., Inc., 1962), Chap. 6.

APPENDIX A.   DISCRETE-ANGLE SOLUTION FOR EVEN-MODE DEFORMATIONS

This appendix details the development of an exact, discrete-angle solution for the radiation pattern of a uniformly illuminated array having even sine-mode deformations. The companion solution for even cosine-mode deformations is also presented.

The principal-plane pattern for a uniformly illuminated, x-directed line source having deformations in the z-direction at the far-field angle θ is

$$V(\theta) = \int_{-L}^{L} \exp\{jk \; [\pm \; x \; \sin\theta + z(x) \; \cos\theta]\} \; dx \qquad (A1)$$

where "+" is for $\phi = 0°$ and "-" is for $\phi = 180°$.

Assuming a $\sin\rho'$ ine-mode deformation and transforming the integration variable to $\eta = r.x$ _ brings the integral into the form

$$V(u) = \frac{2L}{n\pi} \int_{\frac{n\pi}{2}}^{\frac{n\pi}{2}} \exp\left[j\left(\pm \; \frac{2u}{n} \; \eta + \pi u' \; \frac{b_n}{L} \; \sin\eta\right)\right] \; dn \qquad (A2)$$

which is similar to the integral representation of the Bessel function of the first kind and integer order[1]:

$$J_m(z) = \frac{1}{\pi} \int_{0}^{\pi} \cos(z\sin\gamma - m\gamma) \; d\gamma \qquad (A3)$$

In the Bessel function representation, the order m, which corresponds to $\pm 2u/n$ the array pattern expression, is an integer; z, which corresponds to $\pi u'$ b_n/L, is a real number. In the array pattern expression, u is a real function of the far-field angle θ. Therefore, the similarity of the array pattern expression to the Bessel function's representation is valid only for integer values of $2u/n$, or only at discrete angles.

Assume that $\pm 2u/n$ has the integer value m. The array pattern expression, transformed to the Bessel function variables, is

$$V(m,z) = \frac{4L}{n\pi} \int_0^{\frac{n\pi}{2}} \cos(m\eta + z\sin\eta) \, d\eta \qquad (A4)$$

If n is even, Eq. (A5) may be expressed as two sums of $\frac{n}{2}$ integrals:

$$V(m,z) = \frac{4L}{n\pi} \sum_{k=0}^{\frac{n}{2}-1} \cos(mk\pi) \int_0^\pi \cos m\eta \, \cos(z\sin\eta) \, d\eta$$

$$- \frac{4L}{n\pi} \sum_{k=0}^{\frac{n}{2}-1} \cos(mk\pi) \, \cos(k\pi) \int_0^\pi \sin m\eta \, \sin(z\sin\eta) \, d\eta \qquad (A5)$$

These are, in terms of integer-order Bessel functions,[2]

$$V(m,z) = \frac{4L}{n\pi} \sum_{K=0}^{\frac{n}{2}-1} \cos(mk\pi)[1 + (-1)^m] \frac{\pi}{2} (z)$$

$$- \frac{4L}{n\pi} \sum_{K=0}^{\frac{n}{2}-1} \cos(mk\pi) \, \cos(k\pi)[1 - (-1)^m] \frac{\pi}{2} J_m(z) \qquad (A6)$$

The solution for an even-cosine mode is similar. The discrete-angle expressions for the even-sine and even-cosine modes are as follows:

Even-Cosine Modes

$$V(m,z) = \begin{cases} 2L \cos\left(\frac{m\pi}{2}\right) J_m(z), & m \text{ even} \\ j2L \sin\left(\frac{m\pi}{2}\right) J_m(z), & m \text{ odd} \end{cases} \qquad (A7)$$

Even-Sine Modes

$$V(m,z) = \begin{cases} 2LJ_m(z), & m \text{ even} \\ -2LJ_m(z), & m \text{ odd} \end{cases} \tag{A8}$$

These expressions produce exact results for the array pattern at discrete angles. They are useful for measuring the accuracy of approximations of the array pattern, such as the small-amplitude approximation described in Section II.B.1.

APPENDIX A REFERENCES

1. M. Abramowitz and I. Stegun, <u>Handbook of Mathematical Functions</u>
    (Washington, D.C.: Government Printing Office, 1972) (Tenth Printing,
    with corrections), p. 360.

2. I. Gradshteyn and I. Ryzhik, <u>Table of Integrals, Series, and Products</u>
    (New York and London: Academic Press, 1965), pp. 400-402.

APPENDIX B. RADIATION PATTERNS

UNIFORM ILLUMINATION
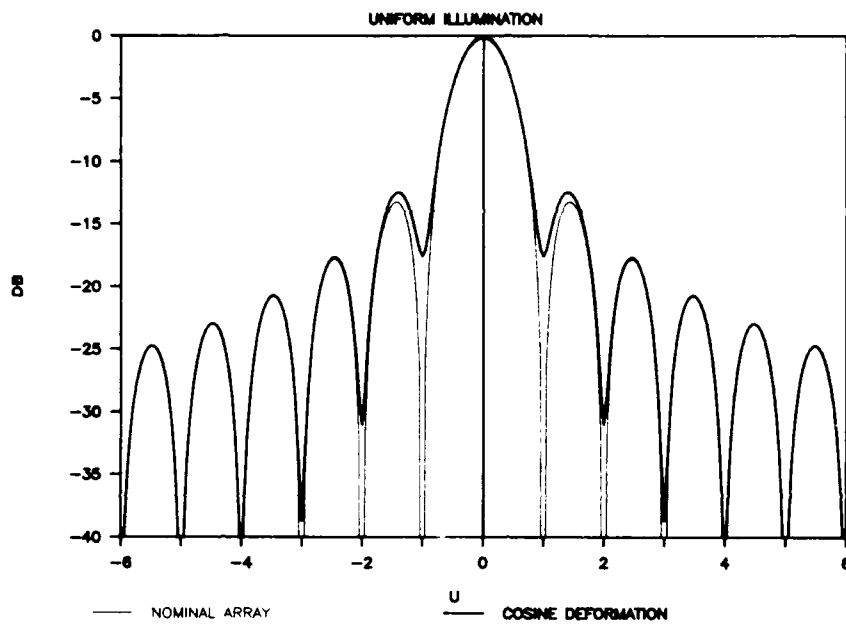
Fig. B1. Mode Order = 1, Mode Amplitude = 0.1 Wavelengths

UNIFORM ILLUMINATION
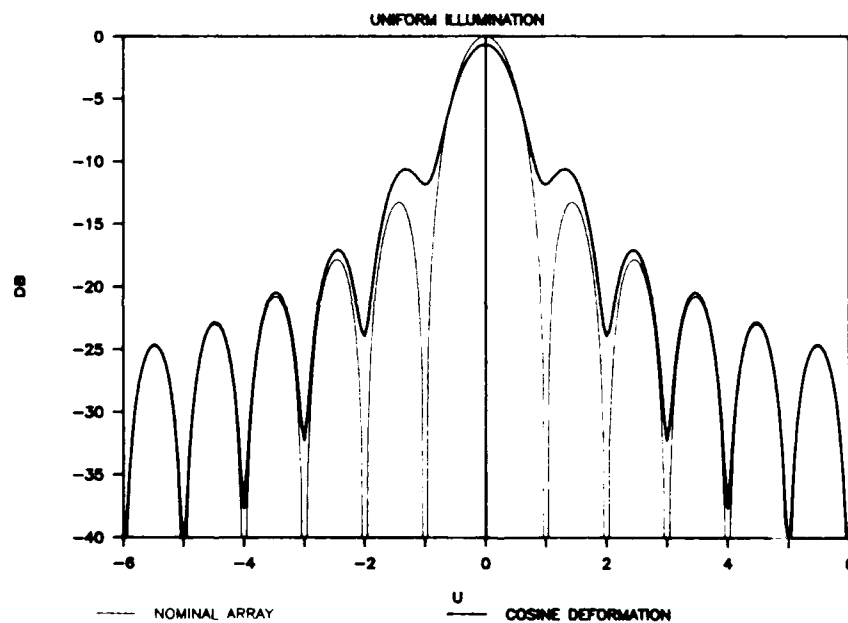
Fig. B2. Mode Order = 1, Mode Amplitude = 0.2 Wavelengths

44
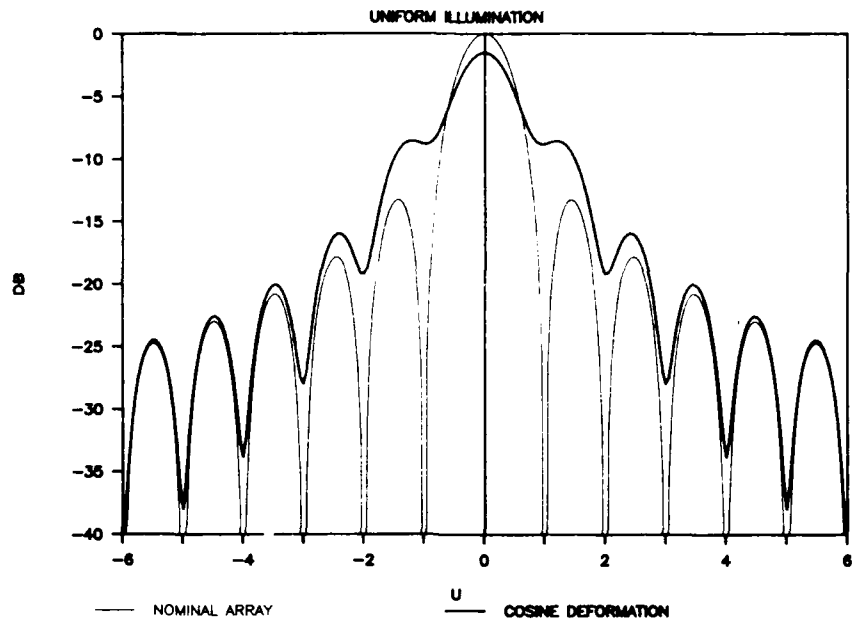
Fig. B3. Mode Order = 1, Mode Amplitude = 0.3 Wavelengths
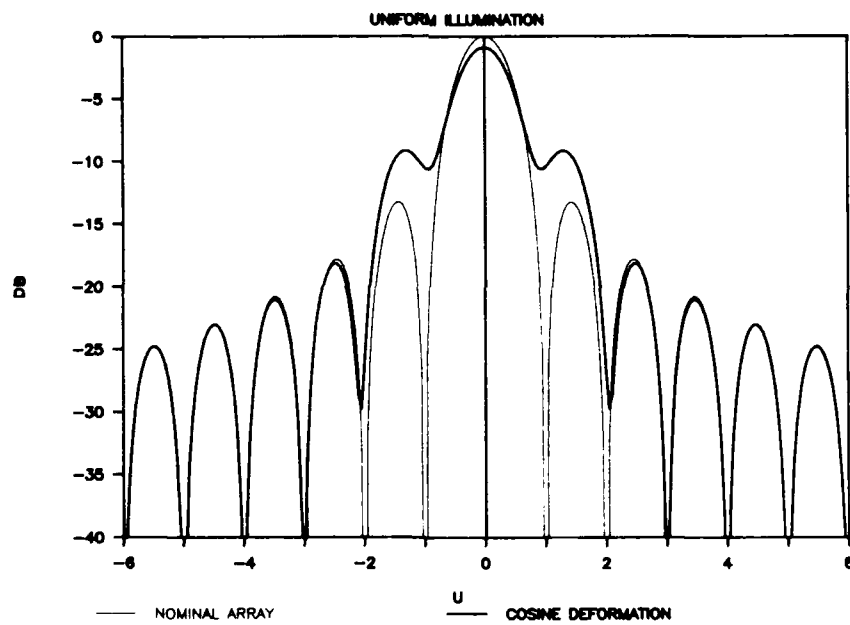
Fig. B4. Mode Order = 2, Mode Amplitude = 0.1 Wavelengths
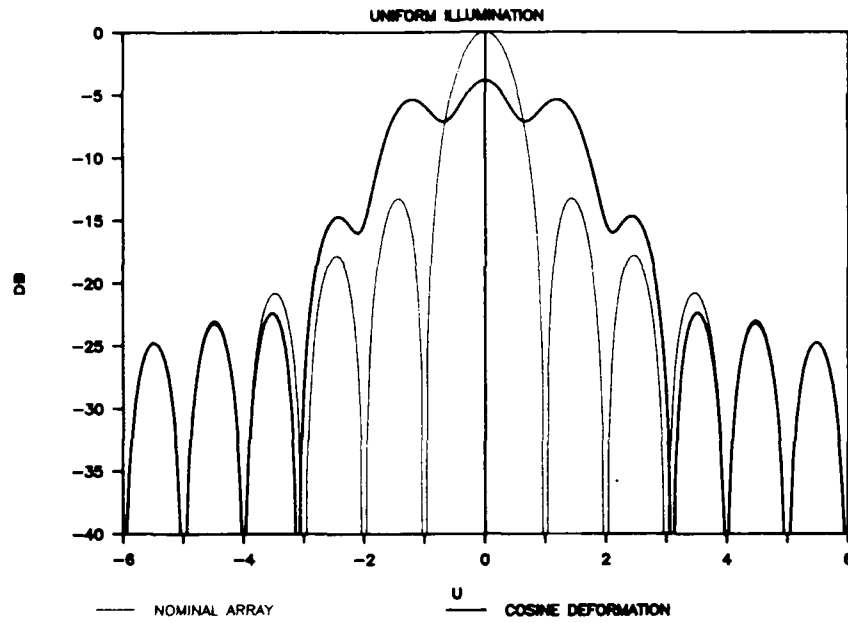
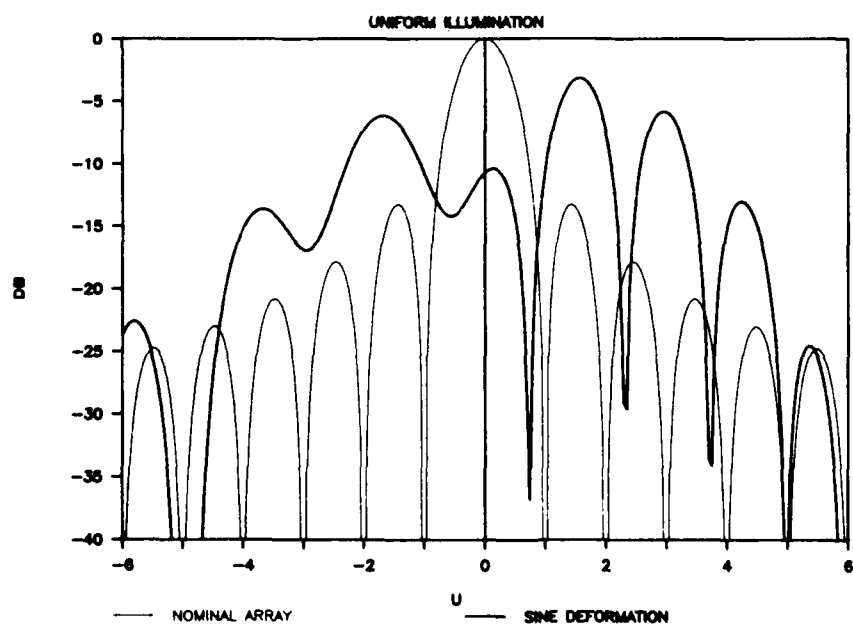Fig. B5. Mode Order = 2, Mode Amplitude = 0.2 Wavelengths
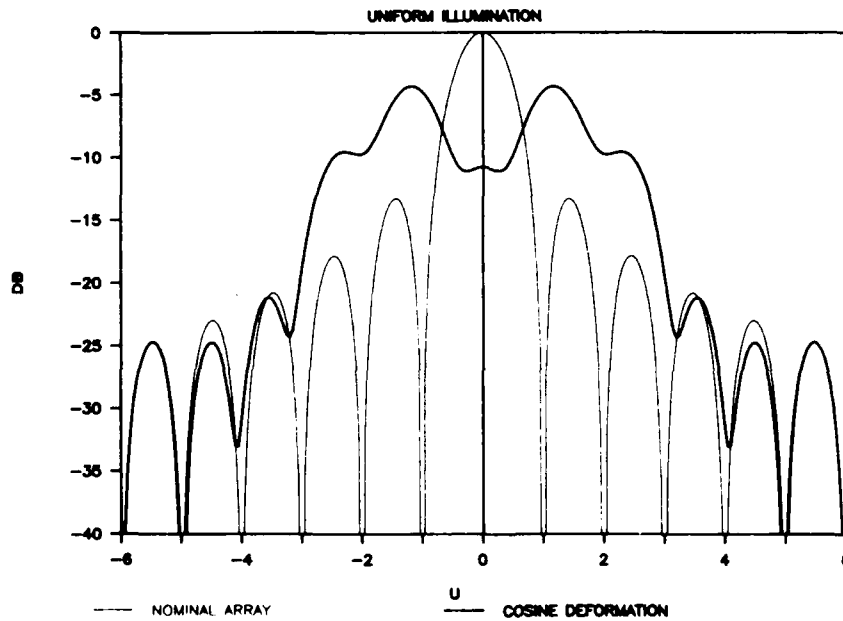
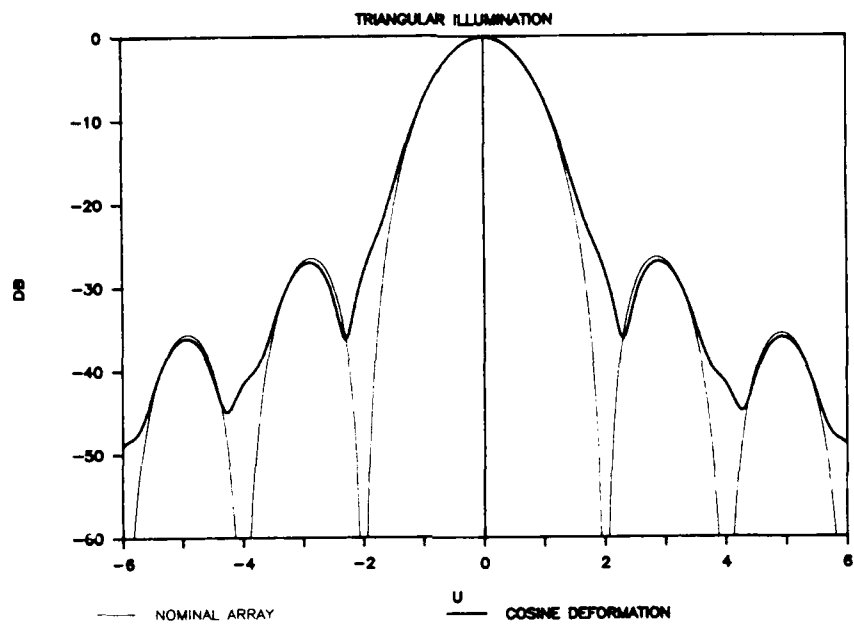
Fig. B6. Mode Order = 2, Mode Amplitude = 0.3 Wavelengths
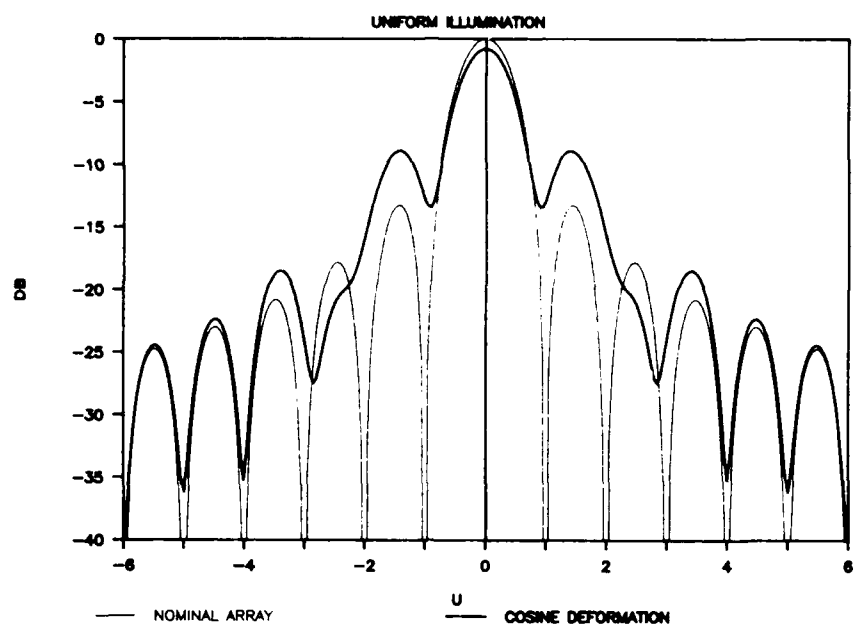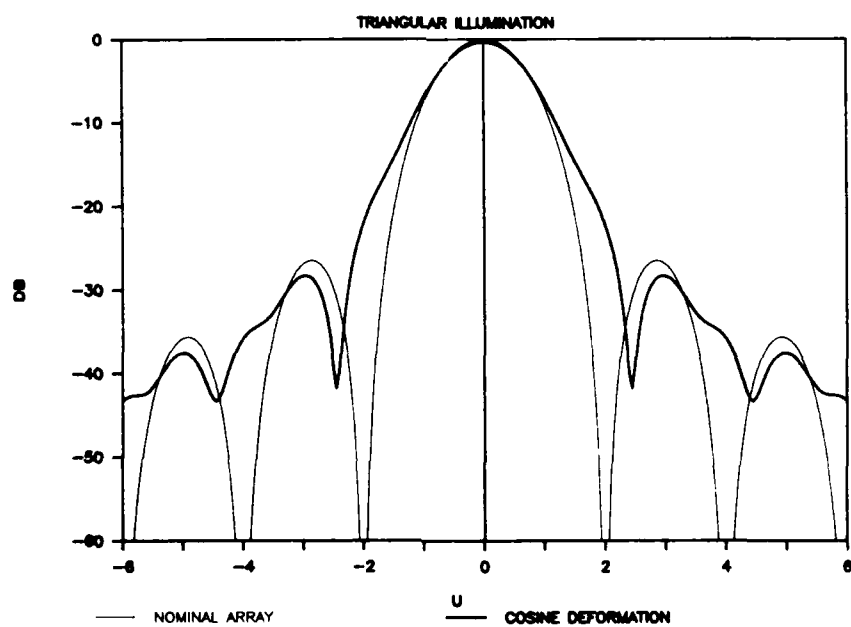
Fig. B7. Mode Order = 3, Mode Amplitude = 0.1 Wavelengths
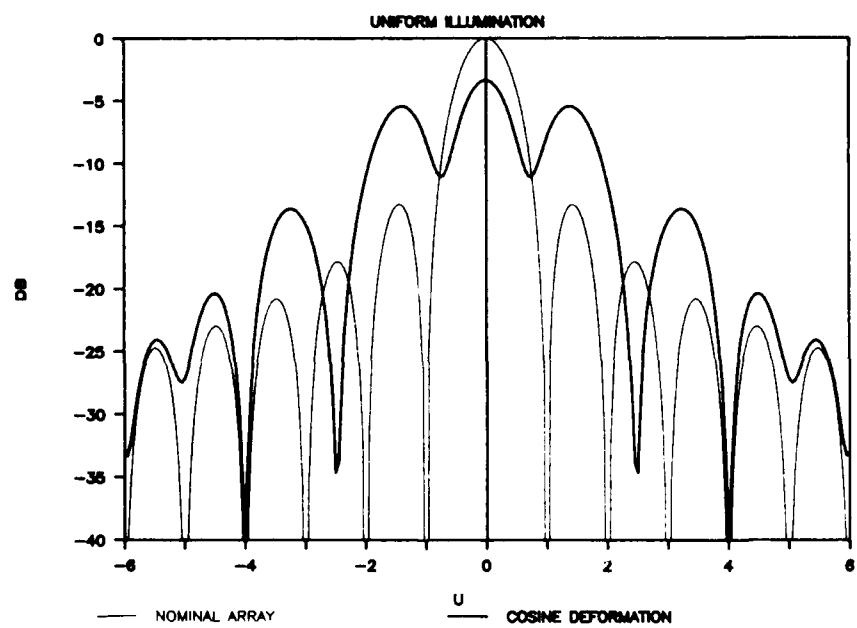
Fig. B8. Mode Order = 3, Mode Amplitude = 0.2 Wavelengths
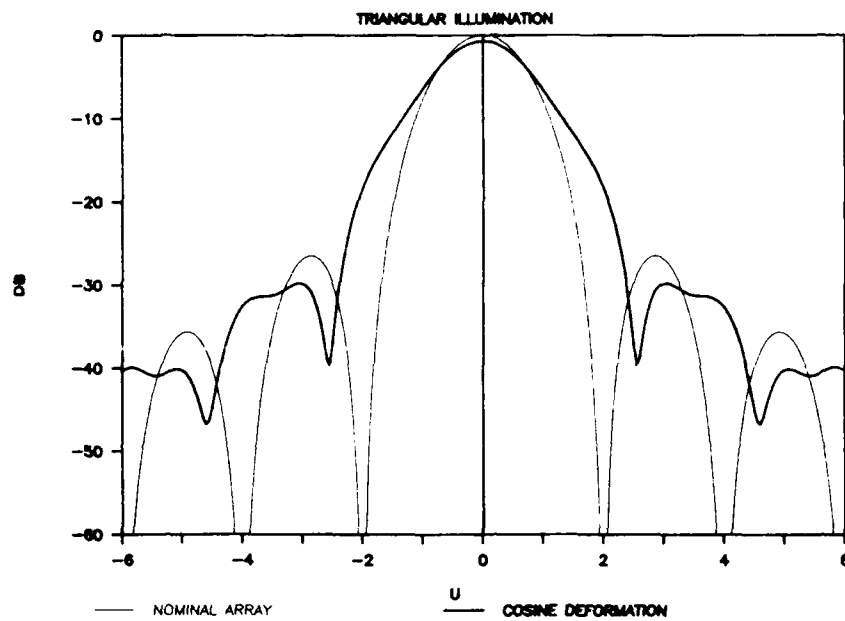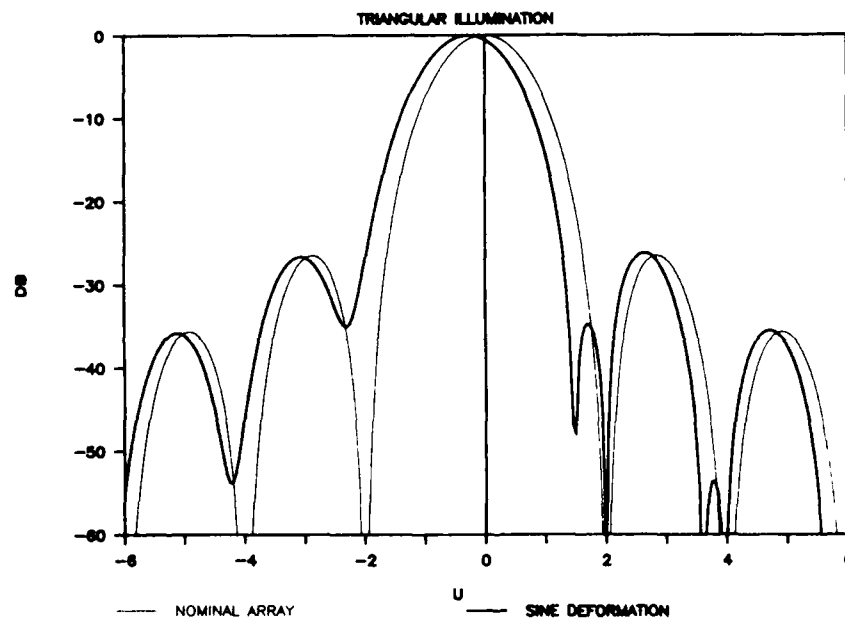
47
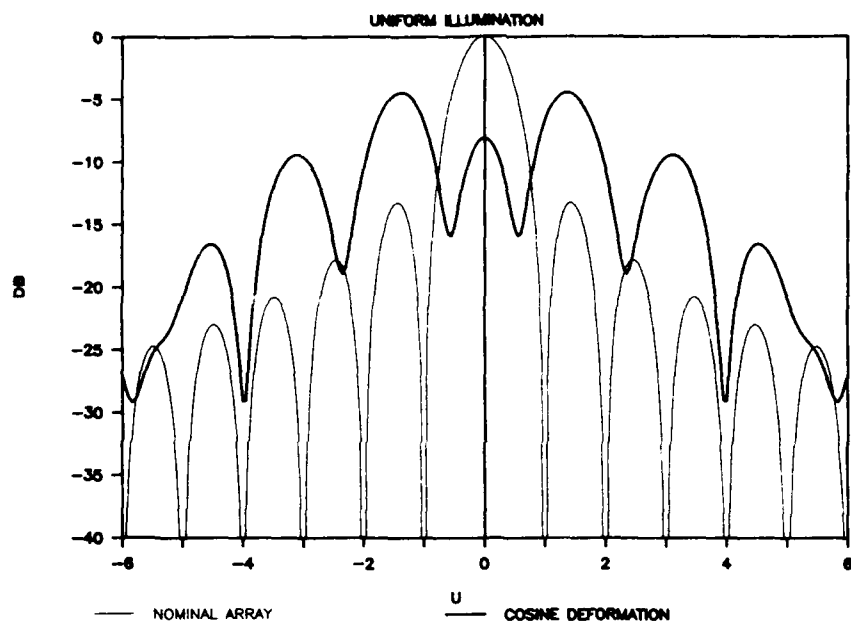
Fig. B9. Mode Order = 3, Mode Amplitude = 0.3 Wavelengths
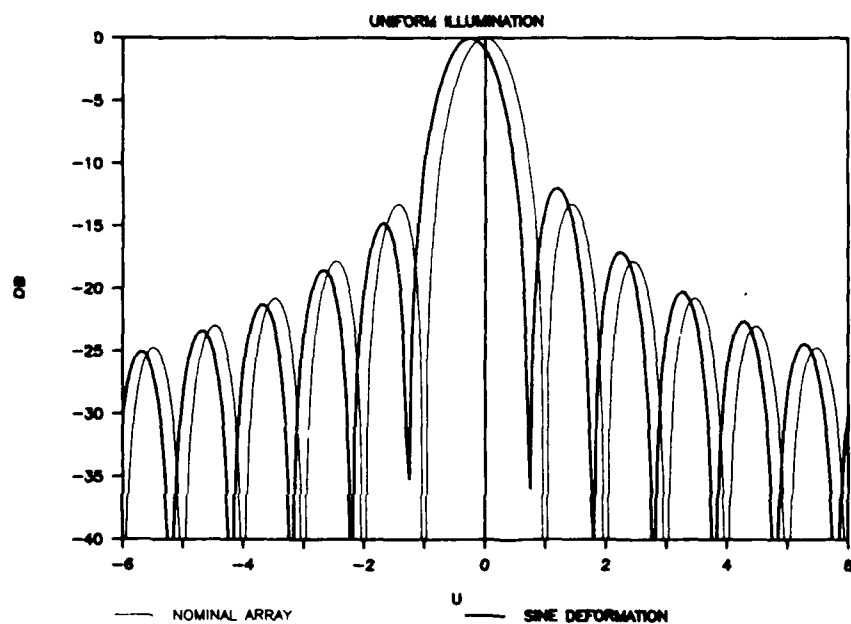
Fig. B10. Mode Order = 1, Mode Amplitude = 0.1 Wavelengths

48
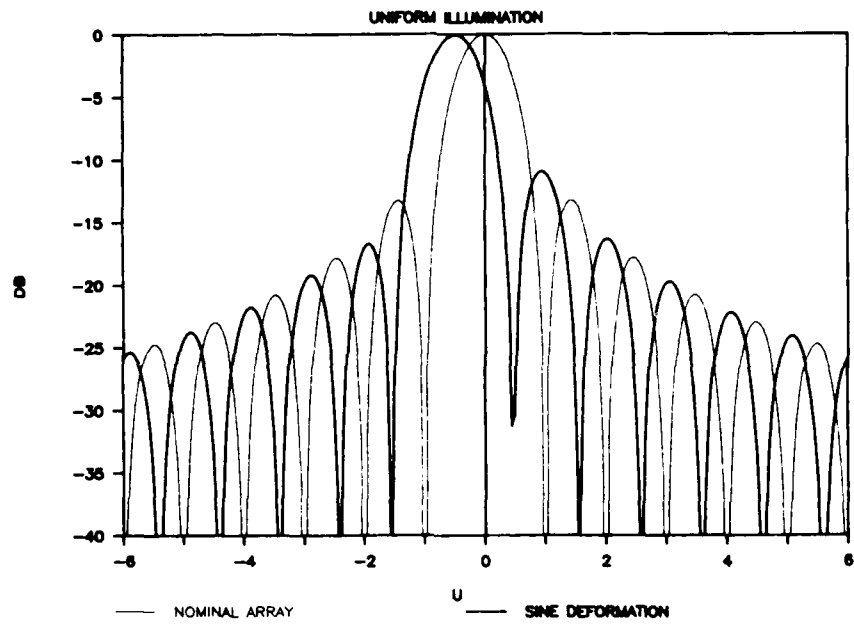
Fig. B11. Mode Order = 1, Mode Amplitude = 0.2 Wavelengths
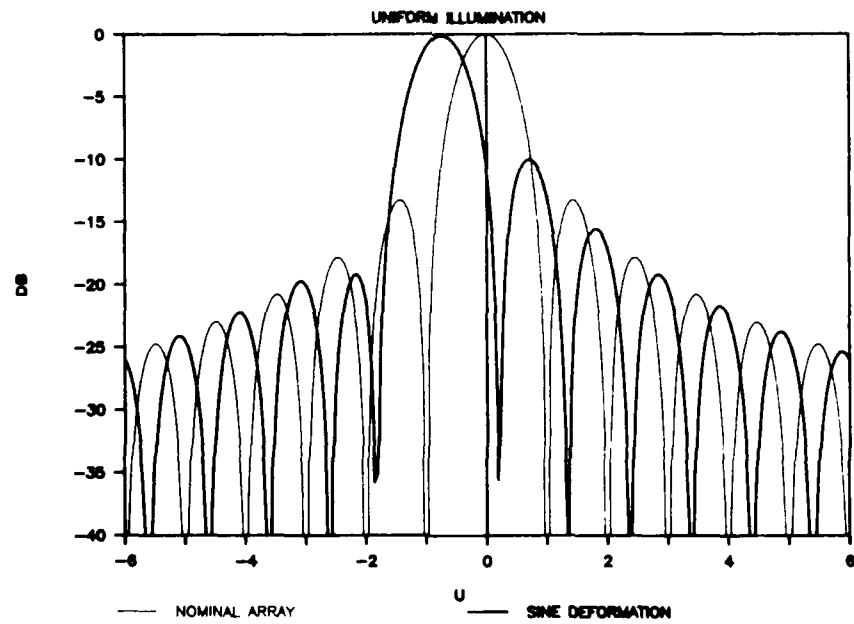
Fig. B12. Mode Order = 1, Mode Amplitude = 0.3 Wavelengths
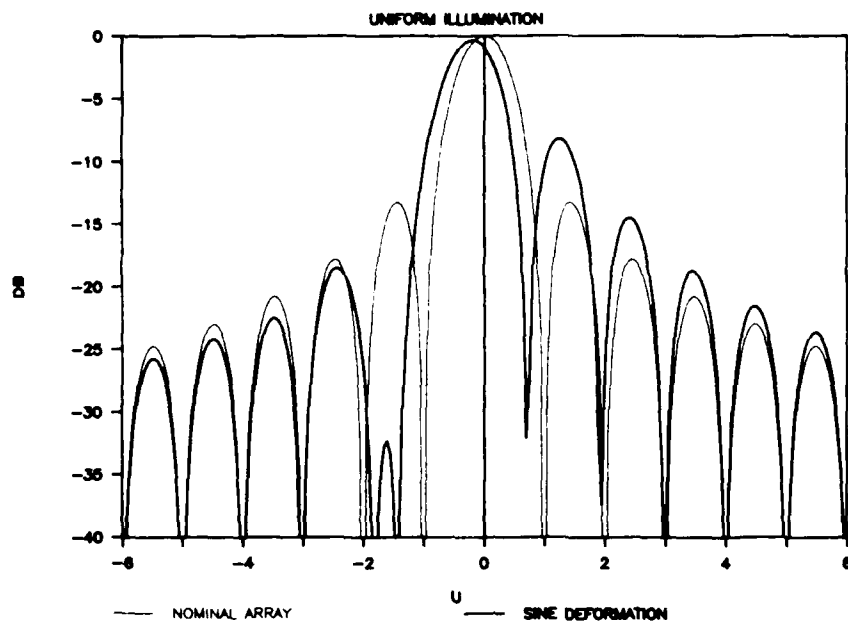
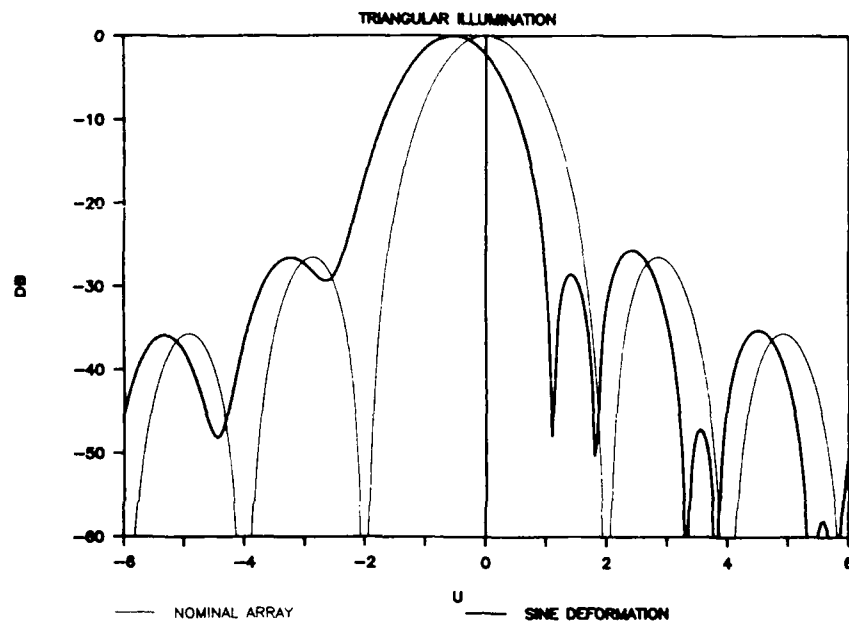Fig. B13. Mode Order = 2, Mode Amplitude = 0.1 Wavelengths
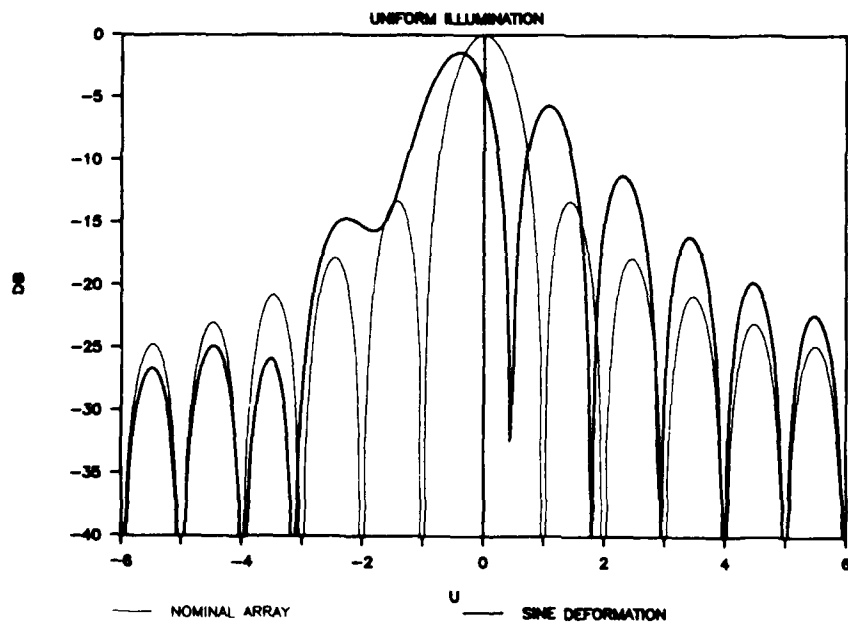
Fig. B14. Mode Order = 2, Mode Amplitude = 0.2 Wavelengths
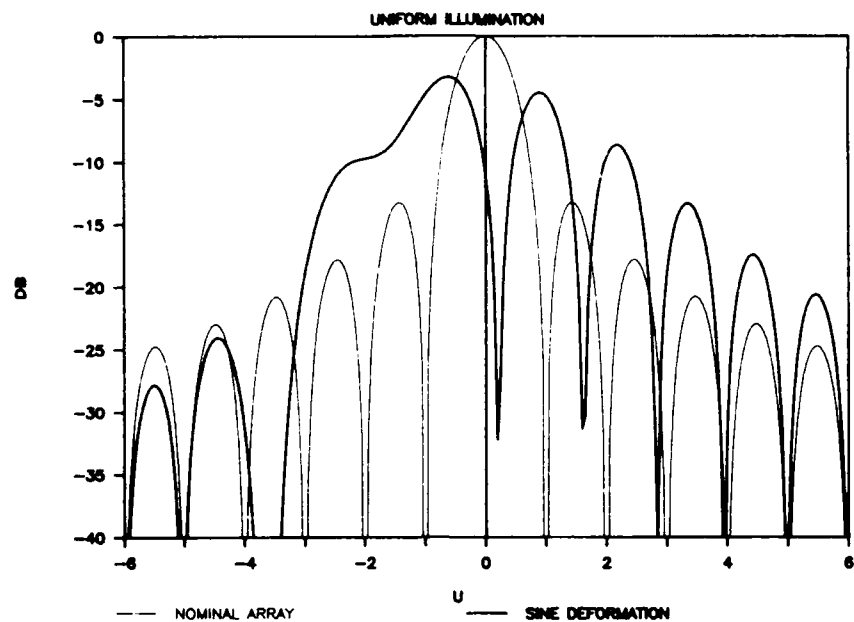
Fig. B15. Mode Order = 2, Mode Amplitude = 0.3 Wavelengths
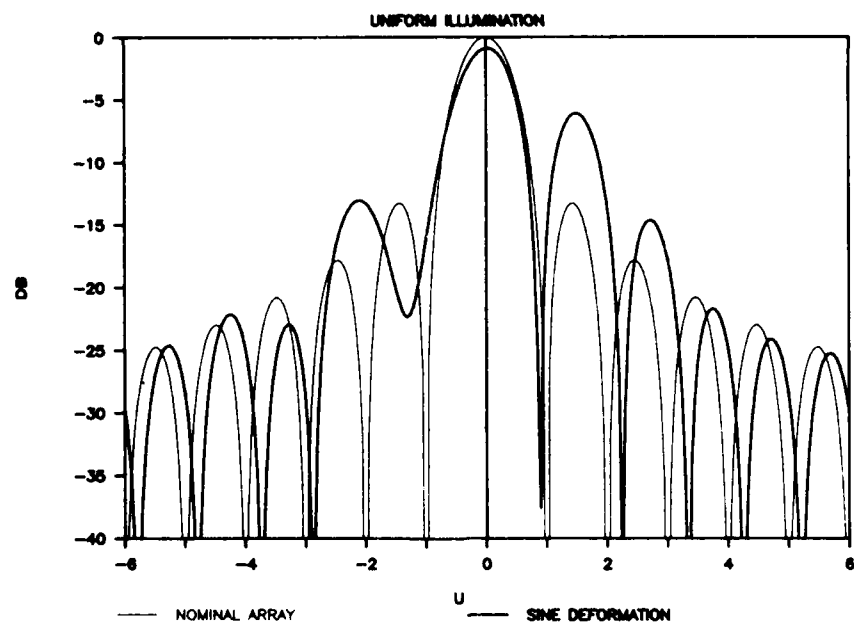
Fig. B16. Mode Order = 3, Mode Amplitude = 0.1 Wavelengths
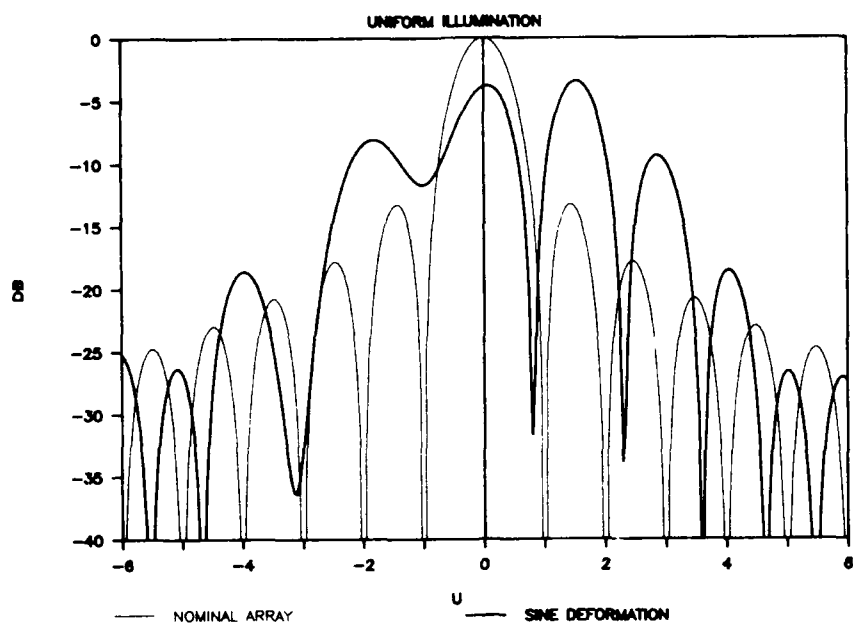
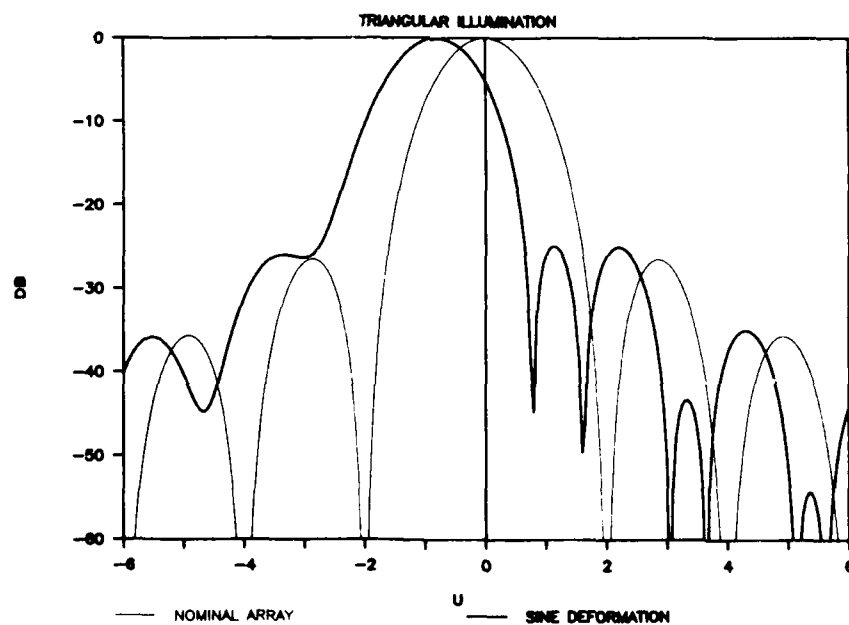Fig. B17. Mode Order = 3, Mode Amplitude = 0.2 Wavelengths

Fig. B18. Mode Order = 3, Mode Amplitude = 0.3 Wavelengths

52

Fig. B19. Mode Order = 1, Mode Amplitude = 0.1 Wavelengths

Fig. B20. Mode Order = 1, Mode Amplitude = 0.2 Wavelengths

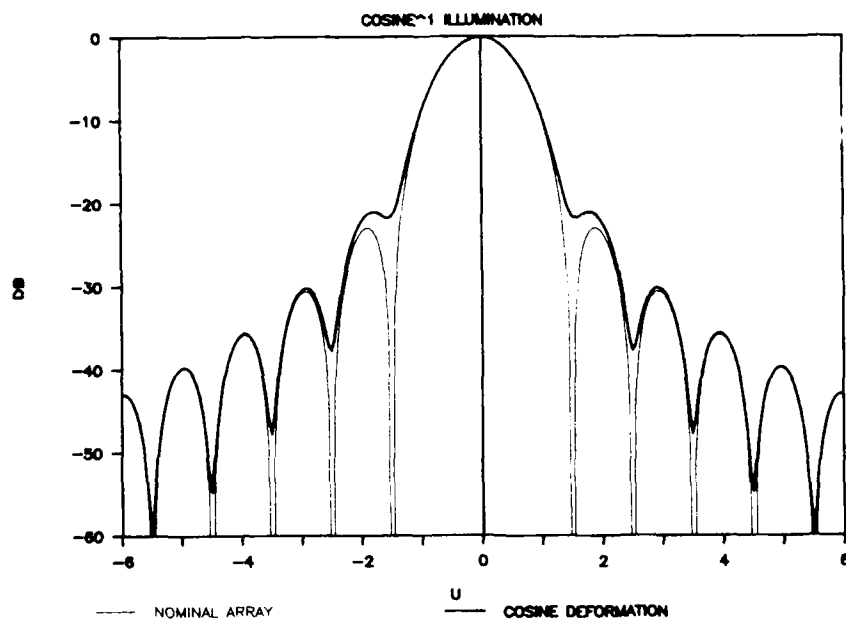Fig. B21.   Mode Order = 1, Mode Amplitude = 0.3 Wavelengths

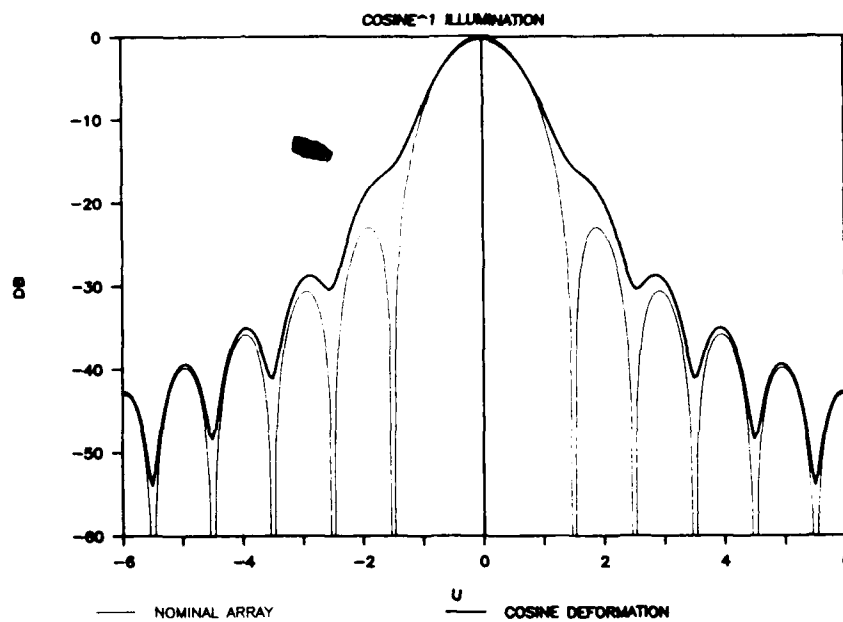Fig. B22.   Mode Order = 1, Mode Amplitude = 0.1 Wavelengths

54

TRIANGULAR ILLUMINATION

NOMINAL ARRAY   U   SINE DEFORMATION

Fig. B23. Mode Order = 1, Mode Amplitude = 0.2 Wavelengths

TRIANGULAR ILLUMINATION

NOMINAL ARRAY   U   SINE DEFORMATION

Fig. B24. Mode Order = 1, Mode Amplitude = 0.3 Wavelengths

Fig. B25. Mode Order = 1, Mode Amplitude = 0.1 Wavelengths

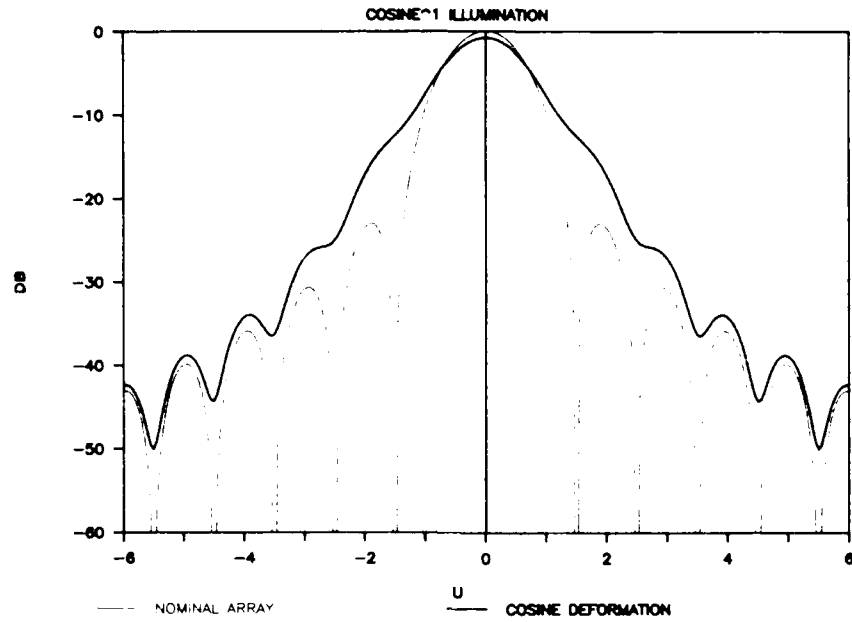Fig. B27. Mode Order = 1, Mode Amplitude = 0.3 Wavelengths

56

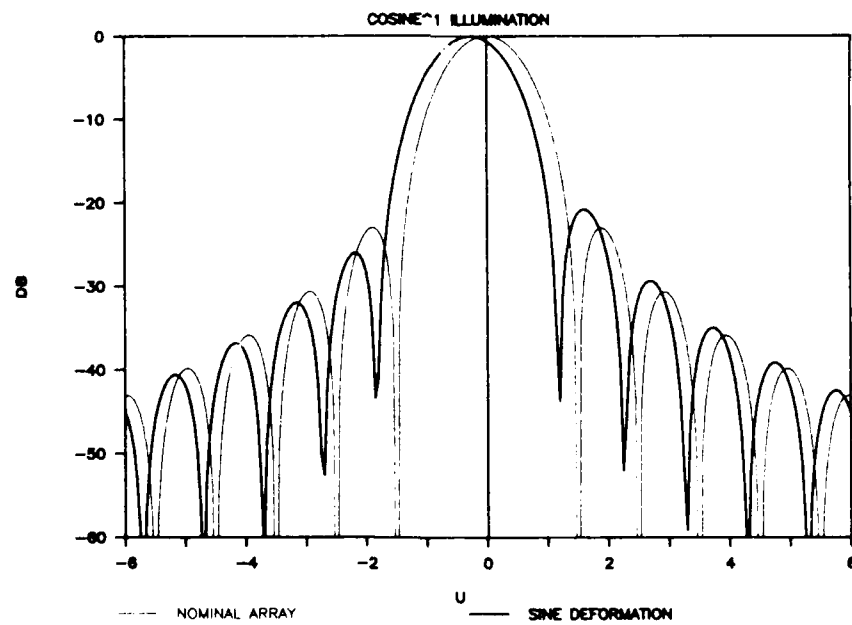Fig. B26. Mode Order = 1, Mode Amplitude = 0.2 Wavelengths

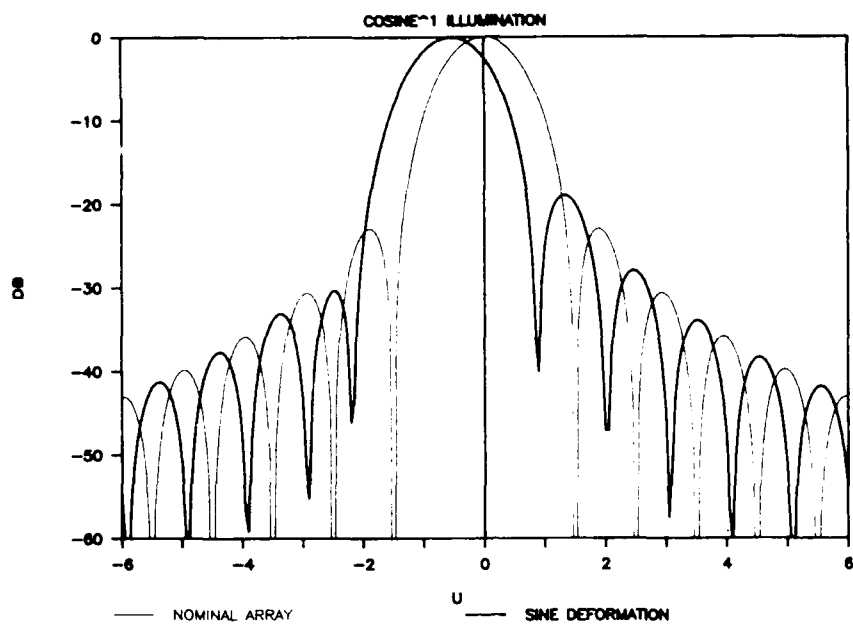Fig. B28. Mode Order = 1, Mode Amplitude = 0.1 Wavelengths

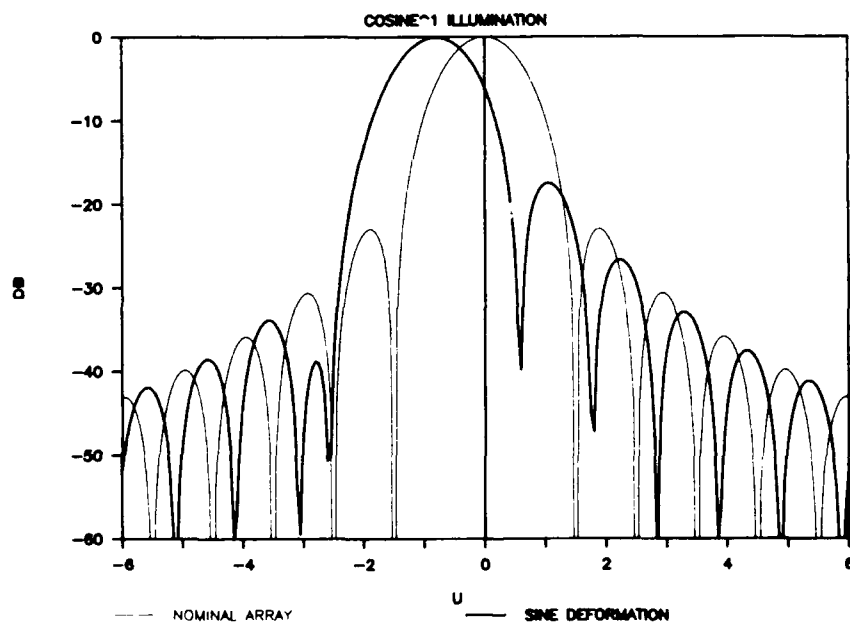Fig. B29. Mode Order = 1, Mode Amplitude = 0.2 Wavelengths

Fig. B30. Mode Order = 1, Mode Amplitude = 0.3 Wavelengths

COSINE^2 ILLUMINATION

Fig. B31. Mode Order = 1, Mode Amplitude = 0.1 Wavelengths

COSINE^2 ILLUMINATION

Fig. B32. Mode Order = 1, Mode Amplitude = 0.2 Wavelengths

59

COSINE^2 ILLUMINATION

— NOMINAL ARRAY   — COSINE DEFORMATION

Fig. B33. Mode Order = 1, Mode Amplitude = 0.3 Wavelengths

COSINE^2 ILLUMINATION
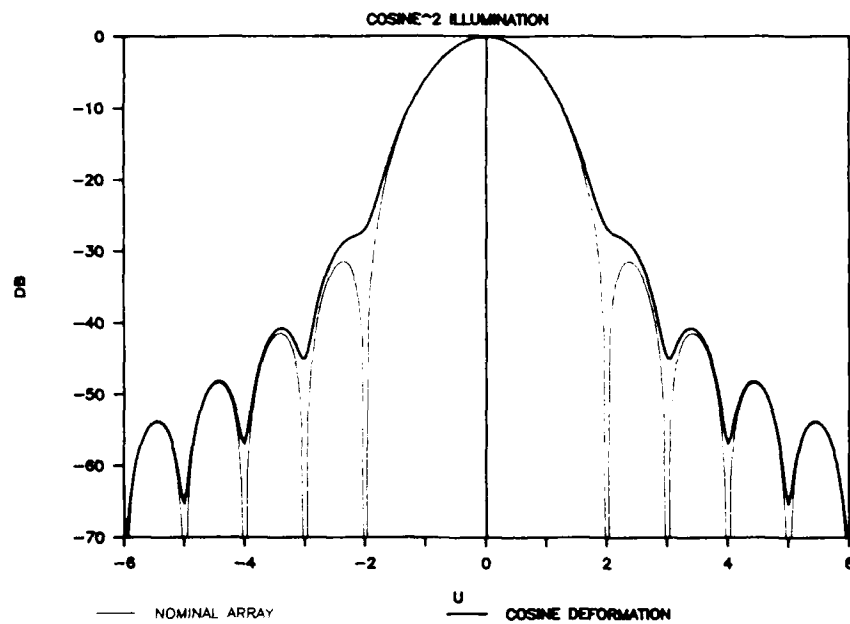
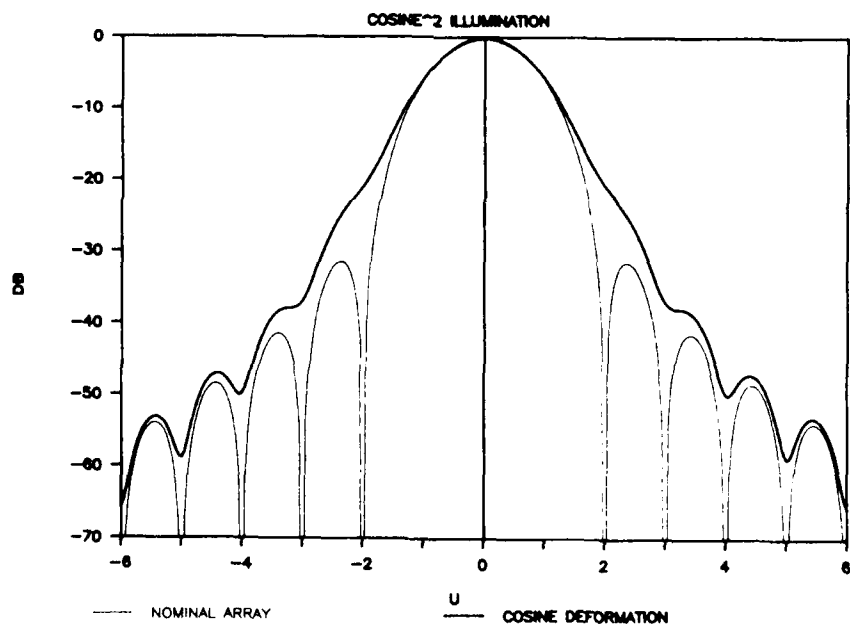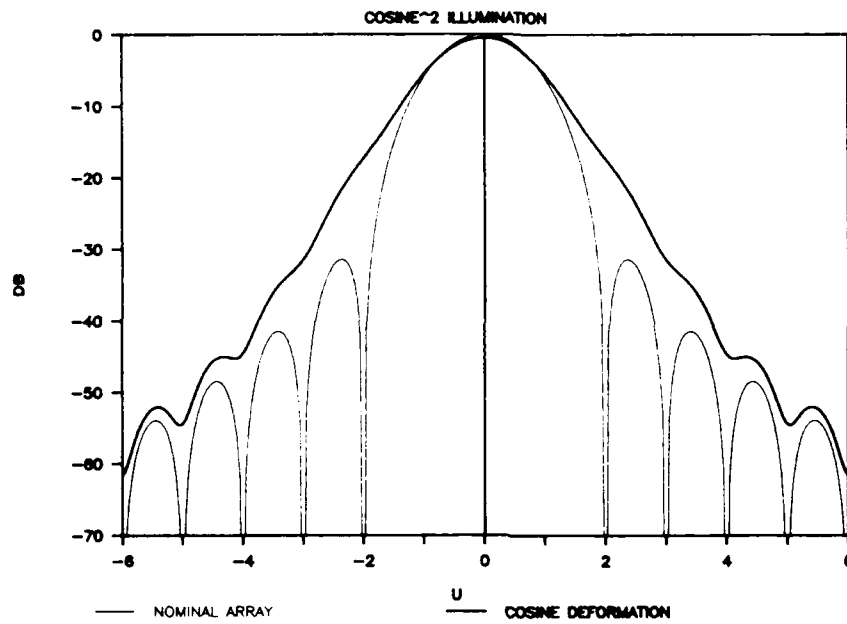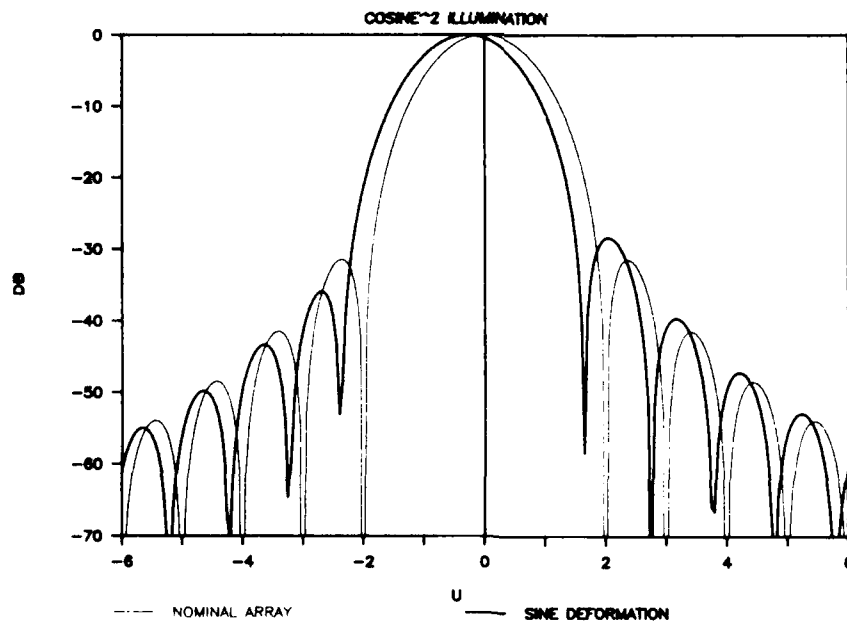—·— NOMINAL ARRAY   — SINE DEFORMATION

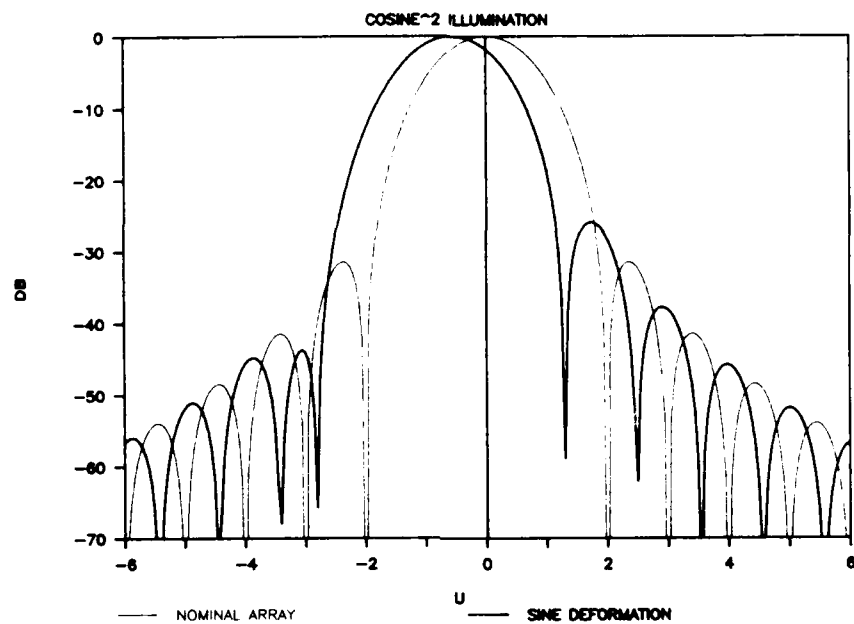Fig. B34. Mode Order = 1, Mode Amplitude = 0.1 Wavelengths

60

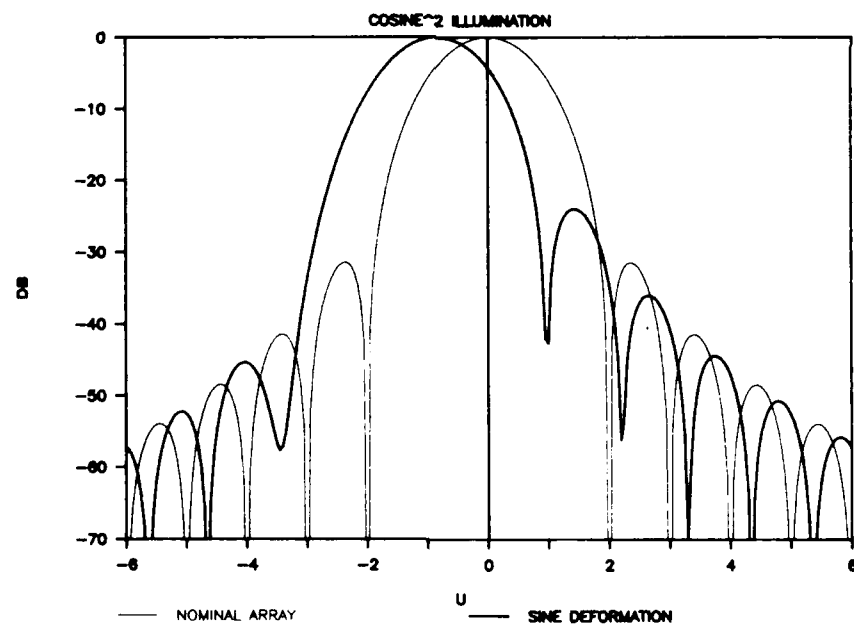Fig. B35. Mode Order = 1, Mode Amplitude = 0.2 Wavelengths

Fig. B36. Mode Order = 1, Mode Amplitude = 0.3 Wavelengths

LABORATORY OPERATIONS

The Aerospace Corporation functions as an "architect-engineer" for national security projects, specializing in advanced military space systems. Providing research support, the corporation's Laboratory Operations conducts experimental and theoretical investigations that focus on the application of scientific and technical advances to such systems. Vital to the success of these investigations is the technical staff's wide-ranging expertise and its ability to stay current with new developments. This expertise is enhanced by a research program aimed at dealing with the many problems associated with rapidly evolving space systems. Contributing their capabilities to the research effort are these individual laboratories:

Aerophysics Laboratory: Launch vehicle and reentry fluid mechanics, heat transfer and flight dynamics; chemical and electric propulsion, propellant chemistry, chemical dynamics, environmental chemistry, trace detection; spacecraft structural mechanics, contamination, thermal and structural control; high temperature thermomechanics, gas kinetics and radiation; cw and pulsed chemical and excimer laser development including chemical kinetics, spectroscopy, optical resonators, beam control, atmospheric propagation, laser effects and countermeasures.

Chemistry and Physics Laboratory: Atmospheric chemical reactions, atmospheric optics, light scattering, state-specific chemical reactions and radiative signatures of missile plumes, sensor out-of-field-of-view rejection, applied laser spectroscopy, laser chemistry, laser optoelectronics, solar cell physics, battery electrochemistry, space vacuum and radiation effects on materials, lubrication and surface phenomena, thermionic emission, photo-sensitive materials and detectors, atomic frequency standards, and environmental chemistry.

Computer Science Laboratory: Program verification, program translation, performance-sensitive system design, distributed architectures for spaceborne computers, fault-tolerant computer systems, artificial intelligence, micro-electronics applications, communication protocols, and computer security.

Electronics Research Laboratory: Microelectronics, solid-state device physics, compound semiconductors, radiation hardening; electro-optics, quantum electronics, solid-state lasers, optical propagation and communications; microwave semiconductor devices, microwave/millimeter wave measurements, diagnostics and radiometry, microwave/millimeter wave thermionic devices; atomic time and frequency standards; antennas, rf systems, electromagnetic propagation phenomena, space communication systems.

Materials Sciences Laboratory: Development of new materials: metals, alloys, ceramics, polymers and their composites, and new forms of carbon; non-destructive evaluation, component failure analysis and reliability; fracture mechanics and stress corrosion; analysis and evaluation of materials at cryogenic and elevated temperatures as well as in space and enemy-induced environments.

Space Sciences Laboratory: Magnetospheric, auroral and cosmic ray physics, wave-particle interactions, magnetospheric plasma waves; atmospheric and ionospheric physics, density and composition of the upper atmosphere, remote sensing using atmospheric radiation; solar physics, infrared astronomy, infrared signature analysis; effects of solar activity, magnetic storms and nuclear explosions on the earth's atmosphere, ionosphere and magnetosphere; effects of electromagnetic and particulate radiations on space systems; space instrumentation.